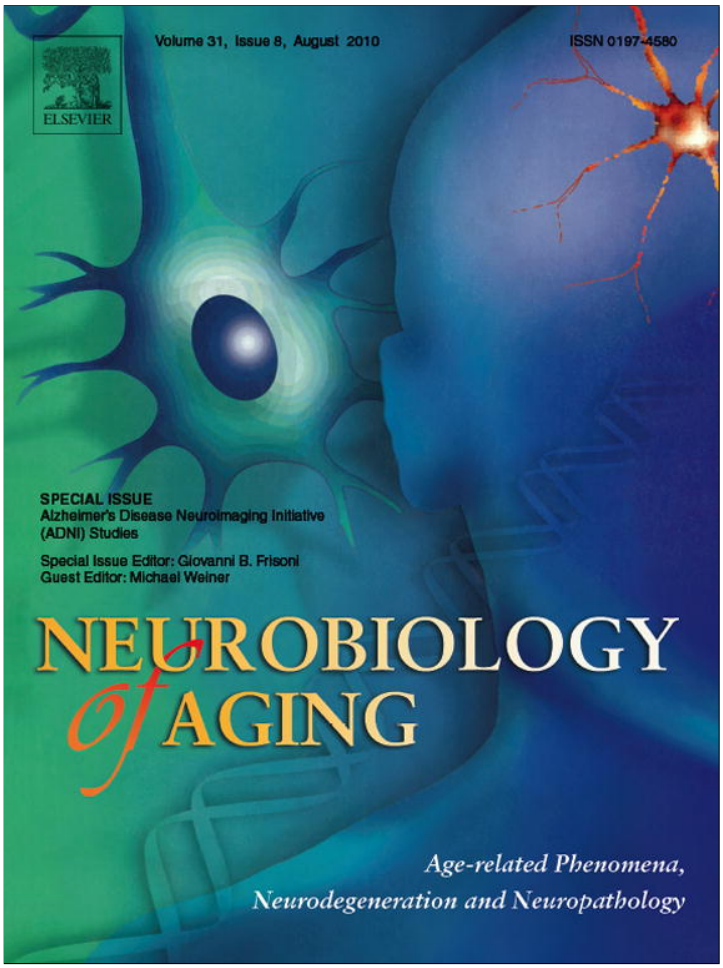

ELSEVIER

Neurobiology of Aging 31 (2010) 1463–1480

NEUROBIOLOGY OF AGING

www.elsevier.com/locate/neuaging

Sex and age differences in atrophic rates: an ADNI study with $n=1368$ MRI scans

Xue Hua [a], Derrek P. Hibar [a], Suh Lee [a], Arthur W. Toga [a], Clifford R. Jack Jr. [b], Michael W. Weiner [c,d], Paul M. Thompson [a,*], and the Alzheimer's Disease Neuroimaging Initiative

[a] *Laboratory of Neuro Imaging, Department of Neurology, UCLA School of Medicine, Los Angeles, CA, USA*
[b] *Department of Radiology, Mayo Clinic, Rochester, MN, USA*
[c] *Departments of Radiology, Medicine, and Psychiatry, University of California, San Francisco, San Francisco, CA, USA*
[d] *Veterans Affairs Medical Center, San Francisco, CA, USA*

Received 10 February 2010; received in revised form 26 April 2010; accepted 27 April 2010

Abstract

We set out to determine factors that influence the rate of brain atrophy in 1-year longitudinal magnetic resonance imaging (MRI) data. With tensor-based morphometry (TBM), we mapped the 3-dimensional profile of progressive atrophy in 144 subjects with probable Alzheimer's disease (AD) (age: 76.5 ± 7.4 years), 338 with amnestic mild cognitive impairment (MCI; 76.0 ± 7.2), and 202 healthy controls (77.0 ± 5.1), scanned twice, 1 year apart. Statistical maps revealed significant age and sex differences in atrophic rates. Brain atrophic rates were about 1%–1.5% faster in women than men. Atrophy was faster in younger than older subjects, most prominently in mild cognitive impairment, with a 1% increase in the rates of atrophy and 2% in ventricular expansion, for every 10-year decrease in age. TBM-derived atrophic rates correlated with reduced beta-amyloid and elevated tau levels ($n = 363$) at baseline, baseline and progressive deterioration in clinical measures, and increasing numbers of risk alleles for the ApoE4 gene. TBM is a sensitive, high-throughput biomarker for tracking disease progression in large imaging studies; sub-analyses focusing on women or younger subjects gave improved sample size requirements for clinical trials.

Keywords: Alzheimer's disease; Mild cognitive impairment; MRI; Longitudinal; Tensor-based morphometry; Age; Sex effect; Atrophy rate; Neuroimaging; Biomarker; Drug trial enrichment

1. Introduction

Alzheimer's disease (AD) is a neurodegenerative disorder characterized by pathologic accumulation of misfolded beta-amyloid (Aβ) peptides in the neuropil, and hyperphosphorylated tau (p-tau) proteins in neurons (Selkoe, 2004; Skovronsky et al., 2006). The macroscopic effects of neuronal atrophy, cell death, and myelin impairment are detectable on high-resolution structural magnetic resonance imaging (MRI), offering an in vivo index of progressive brain deterioration. AD pathology accumulates up to 2 decades before overt cognitive decline, and minimally symptomatic subjects, with mild cognitive impairment (MCI) (Petersen, 2003; Petersen et al., 2001), are a key target in clinical trials (Grundman et al., 2004). Various imaging measures have been proposed as biomarkers of the disease, reflecting different aspects of AD pathology. Efforts are underway to assess their power for diagnosis, predicting future decline, and sensitivity to the effects of potential disease-modifying treatments (Frisoni et al., 2009; Jagust et al., 2009; Shaw et al., 2007).

Longitudinal brain MRI can be used to track disease progression with high precision and statistical power (Hua

* Corresponding author at: UCLA School of Medicine, Laboratory of Neuro Imaging, Departmant of Neurology, Neuroscience Research Building 225E, 635 Charles Young Drive, Los Angeles, CA 90095-1769, United States. Tel.: +1 310 206 2101; fax: +1 310 206 5518.
E-mail address: thompson@loni.ucla.edu (P. Thompson).

0197-4580/$ – see front matter © 2010 Elsevier Inc. All rights reserved.
doi:10.1016/j.neurobiolaging.2010.04.033

et al., 2009; Leow et al., 2006). Brain MRI scans can be analyzed with automated or semi-automated methods to measure hippocampal atrophy (Chetelat et al., 2008; Jack et al., 2004; Morra et al., 2009a, 2009b; Schuff et al., 2009; Thompson, et al., 2004), ventricular enlargement (Carmichael, et al., 2006; Chou et al., 2008, 2009a, 2009b; Jack et al., 2003; Nestor et al., 2008; Thompson, et al., 2004), or whole brain atrophy (Fox et al., 1999, 2000; Sluimer et al., 2008; Smith, et al., 2002, 2004). The trajectory of brain atrophy on structural MRI largely mirrors the anatomical pattern and trajectory of neurofibrillary tangle deposition (Chetelat et al., 2002; Thompson, et al., 2003; Vemuri et al., 2008, 2009; Whitwell et al., 2008), correlates with clinical decline (Evans, et al., 2010; Fox et al., 1999; Hua et al., 2008b; Jack et al., 2009; Leow et al., 2009; Thompson, et al., 2004), and predicts future conversion from preclinical to symptomatic AD (Apostolova et al., 2006; Chetelat et al., 2008; Hua et al., 2008b; Jack et al., 1999; Misra et al., 2009; Risacher et al., 2009; Vemuri et al., 2009), suggesting that MRI measures are useful outcome measures for early diagnosis (Chetelat and Baron, 2003) and clinical trials (Frisoni et al., 2010; Halperin et al., 2009; Hill, 2010; Mueller et al., 2005b, 2006; Shaw et al., 2007).

As AD progresses slowly, drug trials are usually underpowered to detect subtle therapeutic effects in a reasonable time interval, given the high cost of scanning large numbers of subjects. Several sample "enrichment" strategies have been proposed to selectively target subjects most likely to decline based on their genotypes (e.g., ApoE4 carriers, those with abnormal Aβ precursor protein genes, presenilin 1 and 2) (Saunders et al., 1993; Consensus Report, 1998), MRI markers of early AD (e.g., hippocampal or entorhinal atrophy) (Devanand et al., 2007; Du et al., 2001; Frisoni et al., 1999; Jack et al., 2004; Morra et al., 2009b), or cerebrospinal fluid (CSF) biomarker profiles (e.g., Aβ, tau, p-tau) (Clark, et al., 2003; de Leon et al., 2006; Hansson et al., 2006; Ibach et al., 2006), to reduce patient heterogeneity and improve statistical power in trials (Clark, et al., 2008; Frank, et al., 2003; Shaw et al., 2007; Thal, et al., 2006;). If factors influencing atrophic rates were better understood, they could be used, in principle, to stratify cohorts into subgroups of subjects most likely to decline. Sex and age differences in atrophic rates are still poorly understood: atrophic rates may be faster in young versus older MCI subjects (Jack et al., 2008c), and greater atrophy is seen in early- versus late-onset AD (Frisoni et al., 2007). Women may have higher risk of developing AD than men (Gao et al., 1998) and, relative to men, women with AD may suffer from greater cognitive impairments (Bai, et al., 2009; Fleisher et al., 2005; Henderson and Buckwalter, 1994; Moreno-Martinez, et al., 2008), greater functional disability (Dodge et al., 2003), and more frontal metabolic impairment (Herholz et al., 2002). Even so, MRI evidence of a "sexual dimorphism" in AD is still lacking. Most of the studies to date are underpowered, i.e., do not have a large enough sample size to detect a subtle sex effect on atrophic rates.

Here we assessed how brain atrophic rates depend on age and sex, in one of the largest MRI studies to date, in the hope that adjusting for these factors might enhance the power to track brain atrophy and factors that influence it. We related atrophic rates to other AD biomarkers, including Aβ, tau, and hyperphosphorylated tau (p-tau) levels in the CSF. We correlated atrophic rates with well known and candidate risk genes (*ApoE* and *GRIN2b*). We hypothesized that there would be age and sex differences in atrophy rates, in a diffuse pattern throughout the brain. We also attempted to rank the clinical variables in terms of their strength of association with rates of atrophy. We hypothesized that atrophic rates might correlate more strongly with cognitive scores, both at baseline and their rates of decline, than with changes in CSF biomarkers, which have poorer temporal reproducibility. We also explored some implications of these correlations for boosting power in clinical trials.

2. Methods

2.1. Subjects

Baseline and 1-year follow-up brain MRI scans were downloaded from the Alzheimer's Disease Neuroimaging Initiative (ADNI) public database (www.loni.ucla.edu/ADNI/Data) on or before June 1, 2009, and reflect the status of the database at that point; as data collection is ongoing, we focused on analyzing all available baseline and 1-year follow-up scans, together with the associated demographic information, apolipoprotein E (ApoE) genotypes, CSF biomarker measures (for Aβ, tau, p-tau), and clinical and cognitive databased information on functional and behavioral assessments. ADNI is a large 5-year study launched in 2004 by the National Institute on Aging (NIA), the National Institute of Biomedical Imaging and Bioengineering (NIBIB), the Food and Drug Administration (FDA), private pharmaceutical companies and nonprofit organizations, as a $60 million public-private partnership. The primary goal of ADNI has been to test whether serial MRI, positron emission tomography (PET), other biological markers, and clinical and neuropsychological assessments acquired at multiple sites (as in a typical clinical trial), can replicate results from smaller single site studies measuring the progression of MCI and early AD. Determination of sensitive and specific markers of very early AD progression is intended to aid researchers and clinicians to monitor the effectiveness of new treatments, and lessen the time and cost of clinical trials. The Principal Investigator of this initiative is Michael W. Weiner, MD, VA Medical Center and University of California, San Francisco.

We analyzed 1368 brain MRI scans, from 144 probable AD patients (age at baseline: 76.5 $\pm$ 7.4 years), 338 individuals with amnestic mild cognitive impairment (MCI; 76.0 $\pm$ 7.2), and 202 healthy elderly controls (CTL; 77.0 $\pm$

5.1), each scanned twice, 1 year apart. ADNI patients are scanned at other intervals, but here were focused on the 1-year follow-up data, as such an interval is common in clinical trials, and we wanted to focus on an interval over which changes would be readily detectable. All AD patients met NINCDS/ADRDA Alzheimer's Criteria (proposed in 1984 by the National Institute of Neurological and Communicative Disorders and Stroke and the Alzheimer's Disease and Related Disorders Association) for probable AD (McKhann et al., 1984). ADNI inclusion and exclusion criteria (Mueller et al., 2005a, 2005b), are detailed online at www.alzheimers.org/clinicaltrials/fullrec.asp?PrimaryKey=208.

All subjects (n = 684, consisting of 144 AD, 338 MCI, and 202 control subjects) completed thorough clinical and cognitive assessments at the time of baseline scan. During the 1-year follow-up, 660 (122 AD, 336 MCI, and 202 control subjects) completed an additional set of clinical and cognitive tests. Cognitive tests examined here included the Alzheimer's Disease Assessment Scale-cognitive subscale (ADAS-cog), a 70-point scale designed to measure the severity of cognitive impairment; this is currently the most widely used cognitive measure in AD trials (Mohs, 1994; Rosen et al., 1984). It consists of 11 tasks assessing learning and memory, language production and comprehension, constructional and ideational praxis, and orientation. The Mini Mental State Examination (MMSE) provides a global measure of mental status, evaluating 5 cognitive domains: orientation, registration, attention and calculation, recall, and language (Cockrell and Folstein, 1988; Folstein et al., 1975). The Rey Auditory Verbal Learning Test (AVLT) evaluates learning and memory functions by assessing the ability to recall a list of 15 words, both immediately after each of the 5 learning trials (AVLT-5), and after a 30-minute delay (AVLT-del) (Rey, 1964). The Logical Memory (LM) test is a modified version of the episodic memory assessment from the Wechsler Memory Scale-Revised (WMS-R; Wechsler, 1987). Subjects were asked to recall a short story consisted of 25 pieces of information, both immediately after it was read to the subject (LM-im), and after a 30 minute delay (LM-del). Functional and behavioral assessments, analyzed here, included the sum-of-boxes Clinical Dementia Rating (CDR-SB), ranging from 0–18. The CDR-SB measures dementia severity by evaluating patients' performance in 6 domains: memory, orientation, judgment and problem solving, community affairs, home and hobbies, and personal care (Berg, 1988; Hughes et al., 1982; Morris, 1993). Finally, the Functional Assessment Questionnaire (FAQ) summarizes the functional activities of daily living (Pfeffer et al., 1982). Medical histories of cardiovascular, endocrine-metabolic, gastrointestinal disorders, alcohol abuse, drug abuse, and smoking were obtained at the screening visit from the participant and the study partner. Complete details of the ADNI assessments are found in the ADNI Procedures Manual (http://www.adni-info.org/Scientists/Pdfs/adniproceduresmanual12.pdf) and www.adni-info.org.

The study was conducted according to the Good Clinical Practice guidelines, the Declaration of Helsinki, US 21 CFR Part 50-Protection of Human Subjects, and Part 56-Institutional Review Boards. Written informed consent was obtained from all participants.

2.2. CSF biomarkers

CSF samples were obtained from a subset of the ADNI subjects through lumbar puncture, after an overnight fast. Samples collected at various sites were transferred, on dry ice, to the ADNI Biomarker Core Laboratory at the University of Pennsylvania Medical Center. Levels of Aβ 1–42 peptide, total tau, and tau phosphorylated at the threonine 181 (p-tau) were measured in 363 subjects at baseline (83 AD, 173 MCI, and 107 CTL), and in 251 subjects at 1-year follow-up (50 AD, 122 MCI, and 79 CTL).

2.3. Genotyping

ApoE and genome-wide genotyping were performed on DNA samples obtained from subjects' blood. Genomic DNA samples were analyzed on the Human610-Quad BeadChip (Illumina, Inc, San Diego, California) at the University of Pennsylvania (see www.adni-info.org for detailed information on blood sample collection, DNA preparation, and single nucleotide polymorphism [SNP] genotyping methods). We also assessed the effect of a common genetic variant in the GRIN2b gene, a subunit of the N-methyl-D-aspartic acid (NMDA)-type glutamate receptor, at SNP rs-10845840, which we previously found was associated with bilateral temporal lobe volume in a genome-wide study of the ADNI data (Stein et al., 2010) using the Plink software (Purcell et al., 2007). This SNP encodes a polymorphism in the glutamate receptor, and is over-represented in AD versus controls and is associated with cognitive decline (Stein et al., 2010).

2.4. MRI acquisition and image correction

Scans were acquired on 1.5 T magnetic resonance (MR) scanners at 60 sites across the United States and Canada. Although different type of scanners (GE, Siemens, or Philips) and various software platforms were used, a standardized MRI protocol ensured cross-site comparability (Jack et al., 2008a). A typical 1.5 T MR protocol involved a 3-dimensional sagittal MP-RAGE (magnetization prepared rapid gradient-echo) scan with repetition time (TR): 2400 ms, minimum full echo time (TE), inversion time (TI): 1000 ms, flip angle: 8°, 24 cm field of view, and a 192 × 192 × 166 acquisition matrix in the x-, y-, and z-dimensions, yielding a voxel size of 1.25 × 1.25 × 1.2 mm^3, later reconstructed to 1 mm isotropic voxels.

Image corrections were applied using a processing pipeline at the Mayo Clinic, consisting of: (1) correction of geometrical distortion due to gradient nonlinearity (Jovicich

et al., 2006), i.e., "grad warp"; (2) "B1-correction" to adjust for image intensity inhomogeneity due to B1 nonuniformity (Jack et al., 2008a); (3) "N3" bias field correction for reducing residual intensity inhomogeneity (Sled et al., 1998); and (4) geometrical scaling to remove scanner- and session-specific calibration errors using a phantom scan acquired for each subject (Gunter et al., 2006). All original image files as well as all corrected images are available at www.loni.ucla.edu/ADNI/Data.

2.5. Image preprocessing

First, each subject's follow-up scan was linearly registered to their baseline scan, with a 9-parameter (9P) transformation driven by a mutual information (MI) cost function (Collins, et al., 1994), to adjust for linear differences in position and scale across time. 9P registration can correct for scanner voxel size variations in large longitudinal studies involving multiple sites, scanners and acquisition sequences (Clarkson et al., 2009), consistently outperforming 6-parameter (6P) registration in terms of statistical power (Hua et al., 2009; Paling et al., 2004). Second, to account for global differences in brain scale across subjects, the mutually aligned scan pairs were then linearly registered to the International Consortium for Brain Mapping template (ICBM-53) (Mazziotta et al., 2001), applying the same 9P transformation to both mutually aligned scans. Globally aligned images were resampled in an isotropic space of 220 voxels along x-, y- and z-dimensions with a final voxel size of 1 mm^3.

2.6. Tensor-based morphometry (TBM) and 3D maps of atrophic rates

Individual maps of atrophic rates (also known as "Jacobian maps") were derived from a TBM analysis of MRI scans acquired 1 year apart. These maps represent the rates of tissue shrinkage (or CSF space expansion) at each voxel location in the brain. A Jacobian map was created by nonlinearly warping the 1-year follow-up scan to match the baseline scan of the same individual, driven by a mutual information cost function, and a regularizing term called the symmetrized Kullback–Leibler (sKL-MI) distance (Yanovsky et al., 2009). Registration parameters (sigma = 6 and lambda = 8) were chosen based on our earlier optimization study (Hua et al., 2009). A color-coded map of the Jacobian determinants was computed from the gradient of the deformation field to illustrate regions of volume expansion (i.e., with $\det J(r) > 1$), or contraction (i.e., with $J(r) < 1$) (Ashburner and Friston, 2003; Chung et al., 2001; Freeborough and Fox, 1998; Riddle et al., 2004; Thompson, et al., 2000; Toga, 1999) over the 1-year interval, yielding a map that estimates tissue change rates. Jacobian maps were also spatially normalized across subjects by nonlinearly aligning all individual maps to a minimal deformation template (MDT), for regional comparisons and group statistical analysis. The MDT represented the average shape of 40 healthy elderly controls; the procedure to construct the MDT is detailed in Hua et al. (2008a, 2008b). Average maps were computed by taking the mean at each voxel of the Jacobian maps across subjects.

2.7. Statistical analyses

We performed several statistical analyses to assess factors influencing or related to brain atrophic rates in Alzheimer's disease and normal aging. First, general linear regressions were used to investigate the relations between TBM-derived brain atrophic rates and demographic variables, CSF biomarkers, clinical and neuropsychological measures, known risk genes, imminent conversion to AD, and other risk factors. These correlations were subsequently evaluated by cumulative distribution functions (CDF) to determine if they were significant after controlling for multiple comparisons using conventional criteria, inside the whole brain or within the temporal lobes. The CDFs were also used to rank the strengths of correlations within each category, to find out which factors are most strongly associated with the rates of structural brain atrophy. Second, the 3-dimensional map was reduced to a single numerical score, representing the overall atrophic rate for each individual within a region of interest ROI. Third, based on these numerical scores, a power analysis was used to estimate the patient recruitment size for a hypothetical clinical trial of a disease-modifying drug, using structural imaging or other biomarkers as surrogate measures of disease progression.

2.7.1. General linear correlations and cumulative distribution functions (CDF) computed to assess false discovery rates (FDRs)

At each voxel within the brain, correlations were assessed, using the general linear model, between atrophy rates and: (1) demographic variables (age, sex, and education); (2) baseline and 1-year changes in CSF biomarker levels (Aβ, tau, p-tau, and the ratio of tau to Aβ); (3) baseline and 1-year changes in clinical and behavioral measures: (ADAS-cog, MMSE, AVLT, LM, CDR-SB, and Functional Assessment Questionnaire [FAQ]); (4) medical histories of cardiovascular, endocrine-metabolic, and gastrointestinal disorders, as well as information on alcohol abuse, drug abuse, and smoking; (5) body mass index (BMI); (6) AD risk genes (*ApoE4*, and a newly discovered candidate risk gene, *GRIN2b*; Stein et al., 2010). Correlations were assessed within each diagnostic group independently, and in the combined group (of all AD, MCI, and CTL subjects), where appropriate. Binary categorical (or indicator) variables were used to code sex (female sex as 0; male as 1), medical histories (no medical history as 0; present as 1), and conversion to AD (non-converters as 0; converters as 1). Risk genes were coded as 0, 1, and 2 for 0, 1, and 2 risk alleles, respectively, to represent an additive model assuming an equal contribution of each risk allele to brain atrophy. All other covariates were represented as continuous variables. Multiple regressions allowed the fitting of

a number of predictor variables simultaneously. We first examined age and sex effects (independent variables) on atrophic rates (dependent variables), and age and sex were fitted as covariates to adjust the rest of the correlations for these effects.

CDF plots of the regression p values were used to determine the significance and compare the strengths of association (effect sizes) for the various factors that correlated with atrophic rates, inside a predefined region-of-interest (e.g., the temporal lobes or whole brain). CDF plots are commonly used by false discovery rate methods to assign overall significance values to statistical maps (Benjamini and Hochberg, 1995; Genovese et al. 2002; Storey, 2002). A significant correlation is declared if the CDF intersects the $y = 20x$ line (other than at the origin), i.e., critical $p > 0$, as this shows that the volume of suprathreshold statistics is more than 20 times that expected under null-hypothesis (Chou et al., 2009b; Hua et al., 2008a, 2009; Morra et al., 2009b). The critical p value refers to the point at where CDF plot intersects with the line $y = 20x$, and this represents the highest statistical threshold for which at most 5% false positives are expected in the map. This value is generally higher for stronger effect sizes in the maps, but is not defined if no effect is present (i.e., the false discovery rate in the map cannot be controlled). CDFs may also be used to compare effect sizes for different clinical correlations: CDF curves show increasingly strong statistical correlations in rank order from bottom to top, in each graph.

2.7.2. Numerical summaries of atrophy rates derived from a statistically-defined region-of-interest

A statistically-defined region of interest (stat-ROI), based on voxels with significant atrophic rates over time ($p < 0.001$) within a predefined anatomical ROI, was established in a nonoverlapping training set of 20 AD patients (age at baseline: 74.8 ± 6.3 years; 7 men and 13 women) scanned at baseline and at 1 year. The anatomical ROIs included the whole brain gray matter and temporal lobes, two of the best search regions giving the highest statistical power in tracking AD progress (Hua et al., 2010). This procedure is detailed in Chen et al. (2009), Hua et al. (2009, 2010), and Ho et al. (2009). A numerical summary of the atrophic rate in the whole brain gray matter, or temporal lobe, was computed by taking the arithmetic mean of Jacobian values within the corresponding stat-ROI (Ho et al., 2009; Hua et al., 2009, 2010), giving a single rate of atrophy score for each individual.

2.7.3. Power analysis and sample size estimates

A power analysis was defined by the ADNI Biostatistics Core to estimate the sample size required to detect, with 80% power, a 25% reduction in the mean annual change, as captured by imaging, clinical, or CSF biomarker measures, using a 2-sided test and standard significance level ($\alpha = 0.05$) for a hypothetical 2-arm study (treatment vs. placebo). The estimated minimum sample size for each arm was computed with the formula below. Briefly, β denotes the estimated annual change (average of the group) and σ_D refers to the standard deviation of the rate of atrophy across subjects.

$$n = \frac{2\hat{\sigma}_D^2 \left(z_{1-\alpha/2} + z_{power}\right)^2}{\left(0.25\hat{\beta}\right)^2}$$

Here z_α is the value of the standard normal distribution for which $P[Z < z_\alpha] = \alpha$ (Rosner, 1990). The sample size required to achieve 80% power was computed, denoted by n80. The 95% confidence interval for the n80 statistic was computed based on 10,000 bootstrapped resamplings, with a bias-corrected and accelerated percentile method (Davison and Hinkley, 1997; Efron and Tibshirani, 1993).

3. Results

3.1. Age and sex effects in atrophy rates

The rates of atrophy (Jacobian values) at each location inside the brain were tested for correlations with age and sex in AD, MCI, and CTL groups independently, as well as in the combined group (ALL). The CDF plots (Fig. 1a and b) show that age and sex correlate with atrophic rates, especially in the MCI group, and when all subjects were combined. There was no systematic age difference between the 3 diagnostic groups (mean age was 76.5, 76.0, and 77.0 for AD, MCI, and CTL respectively), so these effects are driven by differences in age within the diagnostic groups, not between them. Comparing CDF curves of the same color — for the whole brain versus temporal lobes — gives a clear impression of the power gained by restricting analyses to regions that are known to change the most. For example, the black curves show that age and sex effects are detected with greater effect sizes when focusing on the temporal lobes, as the CDF curves have a steeper gradient at the origin. They also cross the reference line $y = 20x$ at a higher point, which means that a higher threshold (critical p value or C.P.) can be applied to the statistical maps while keeping the false discovery rate to 5% of the voxels shown.

The sign of the correlations with age — positive inside tissues and negative in the CSF — indicates faster brain degeneration in younger MCI subjects (Fig. 1c), about 1% increase in atrophic rates and 2% increase in ventricular expansion rates for every 10-year decrease in age; AD patients showed a similar but lesser age effect. Healthy controls showed a small but significant age effect in the opposite direction: a few voxels in the CSF and at the boundary of gray matter and CSF showed positive correlations, i.e., younger age is associated with less ventricular expansion. Atrophic rates were faster in women than men by about 1%–1.5% per year, signified by positive correlations between the atrophic rates and sex (female sex was coded arbitrarily as 0; male as 1; Fig. 1d). As expected, the

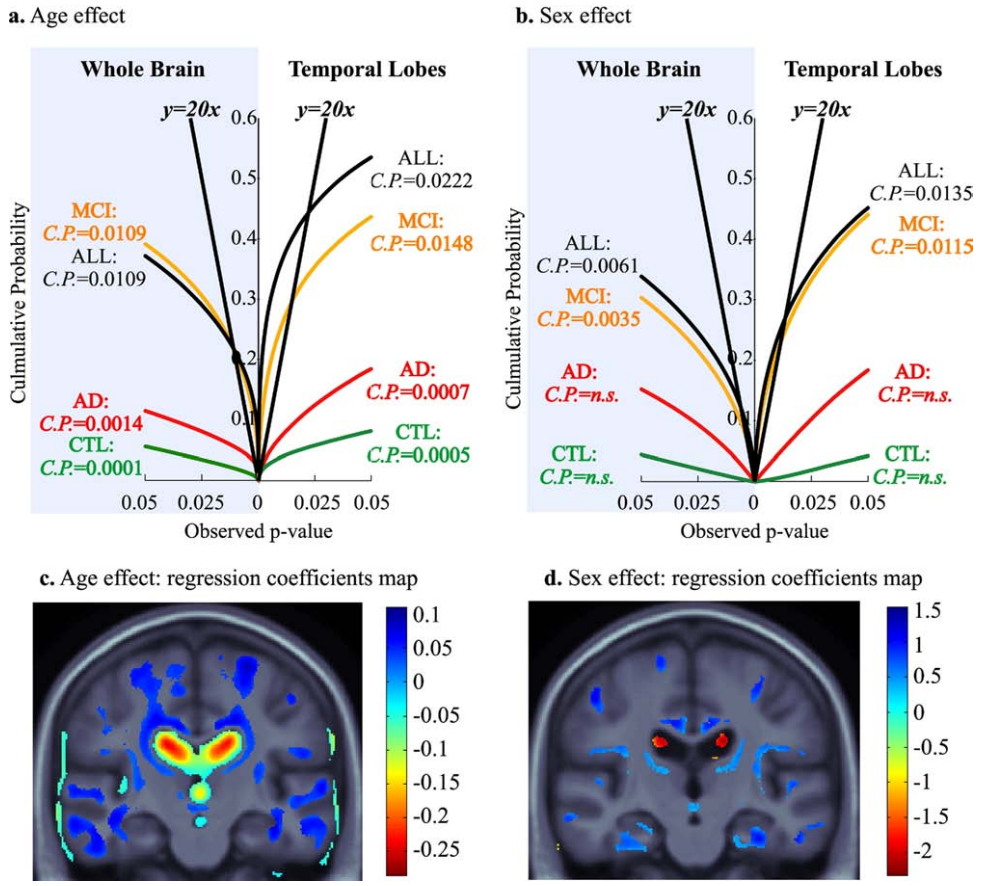

Fig. 1. Age and sex differences in atrophic rates are shown across the entire brain and also in an analysis restricted to changes within the temporal lobes. Cumulative distribution function (CDF) plots for the effects on atrophic rates of age (a) and sex (b) show the statistical significance of their correlations with atrophy rates. Both effects were most prominent in the mild cognitive impairment (MCI) group, probably because it had the most subjects. CDF plots for the whole brain were reflected in the *y* axis to avoid clutter. CDF curves that rise more steeply at the origin generally indicate greater effect sizes. Tests for age and sex effects throughout the whole brain showed inferior statistical power relative to similar tests for effects inside the temporal lobes. This can be seen by comparing CDF curves of the same color in (a) and (b). Regression coefficient maps are shown for the age (c) and sex (d) effects in MCI across the entire brain; colors show the signs of the regression coefficients. The map of each effect (age, sex) is adjusted for the effect of the other covariate. Younger age (↓) is associated with faster tissue loss rates (↓) and faster ventricular expansion (↑). There is approximately a 1% increase in atrophic rates and 2% increase in ventricular expansion rates, for every 10-year decrease in age, as shown by positive correlations in the temporal lobes and negative correlations in the CSF, respectively. Women (↓) had faster brain degeneration (↓) by about 1%–1.5% per year relative to men. These correlation coefficient maps show only the values in regions demonstrating significant correlations, after FDR correction across the entire brain. AD, Alzheimer's disease; MCI, mild cognitive impairment; CTL, healthy elderly controls; ALL, all subjects including AD, MCI, and CTL; C.P., critical *p* value; *n.s.*, not significant.

regression coefficient maps, using thresholds derived within the temporal lobes or across the entire brain, are generally consistent in their spatial distributions. However, a broader area reaches significance if restricting the search region to the temporal lobes, as the critical *p* values are higher within the temporal lobes than those from the whole brain (results not shown).

When we added education and BMI into this regression model, they did not show significant correlations in any group so were not pursued further as confounds. To better illustrate the age and sex differences in atrophic rates, the MCI group was divided into 6 subgroups (in age brackets: 60 to <70, 70 to <80, and 80 to <90 years; further split by sex into female and male). Fig. 2 shows the age and sex effects in a straightforward fashion, as group average maps. The rest of correlations tested in this paper were all statistically adjusted for these effects of age and sex.

As a related question, one might also wonder if age and sex differences were present in the baseline MRI measures. In fact, there were significant age and sex differences in baseline temporal lobe atrophy, within each group independently and in the combined group.

3.2. Correlations between atrophic rates and clinical (cognitive/behavioral) measures

Temporal lobe atrophy rates were correlated with baseline clinical measures (Fig. 3) and with their rates of decline (Fig. 4). In AD and MCI, atrophic rates were most strongly

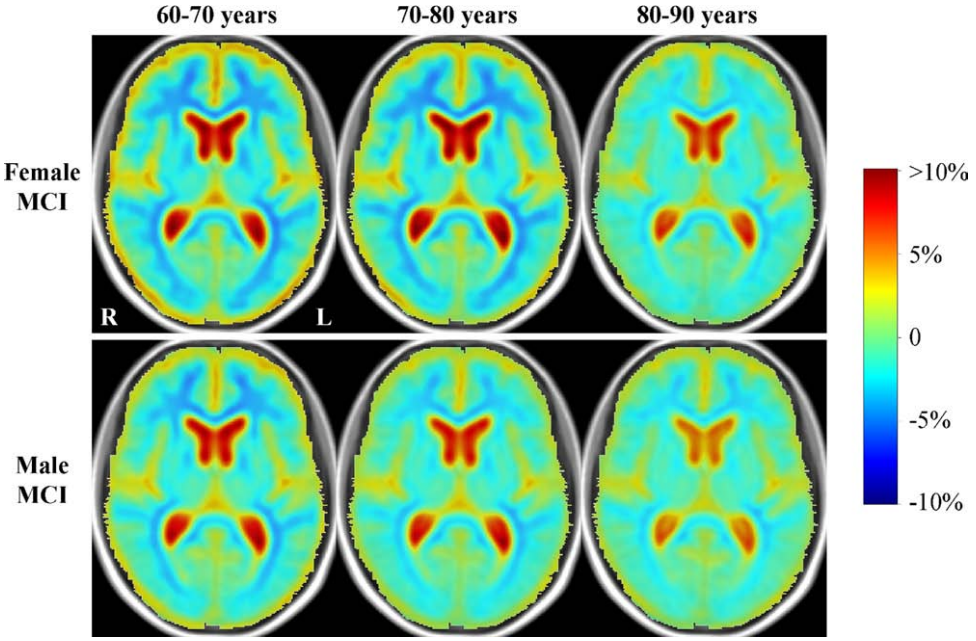

Fig. 2. Average maps of atrophic rates in mild cognitive impairment (MCI) subjects, subdivided by age and sex. Female MCI subjects (top) are divided into 3 age groups, 60–70 (n = 24), 70–80 (n = 59), and 80–90 years (n = 37). Male MCI subjects (bottom) are divided into the age groups of 60–70 (n = 33), 70–80 (n = 102), and 80–90 years (n = 77). Faster atrophic rates occur (darker blue) in younger subjects, and in women versus men; age and sex effects are clearly visible. A small number of MCI subjects (n = 6) fell outside of these age ranges but were too few to form a separate sample so they are not included in the maps.

correlated with the ADAS-cog, LM-im, and AVLT-5 scores at baseline (Fig. 3a and b). Baseline LM-del, AVLT-del, FAQ, and MMSE also showed significant correlations in MCI (Fig. 3b). Anatomical changes over time were also highly correlated with ongoing changes in LM-del, ADAS-cog, CDR-SB, in AD, and CDR-SB, FAQ, LM-im, ADAS-cog, LM-del, in MCI (Fig. 4). The rank order — from highest to lowest effect sizes — is shown for these correlations, with baseline ADAS-cog showing the highest correlations with future atrophic rates. The highest curves show the covariates that are most strongly correlated with the measured atrophic rate.

Similar but weaker effect sizes (lower CDF curves and critical p values) were obtained when expanding the search region to the entire brain, relative to restricting to the temporal lobes, comparing curves of the same color on each side of the plot (Figs. 3 and 4). Using the whole brain ROI, atrophic rates were only significantly correlated with the ADAS-cog at baseline in AD, and baseline measures of ADAS-cog, AVLT-5, LM-del, LM-im, and MMSE in MCI (Fig. 3). Likewise, with the whole brain ROI, atrophic rates were only linked to LM-del decline over a year in AD, while the effect sizes were substantially reduced in MCI (Fig. 4). These "butterfly plots" show that there is a clear boosting of power for detecting statistical effects on atrophy when focusing on the regions where greatest changes are expected (i.e., the temporal lobes).

3.3. Correlating atrophic rates with CSF biomarkers

Rates of brain atrophy were significantly correlated with CSF biomarker levels — Aβ, tau, p-tau, and tau/Aβ — at baseline in the combined group of all subjects (blue CDF curves in Fig. 5). These correlations did not reach statistical significance within each diagnostic group independently, except that the level of CSF Aβ showed weak but significant correlations (critical p = 0.004 in the temporal lobes and 0.001 in the whole brain) in MCI (cyan CDF curves in Fig. 5). Also, there were no detectable correlations between rates of tissue atrophy and the rates of change in the CSF biomarkers within the individual groups, with the exception of tau/Aβ in the whole brain in AD (critical p = 0.003). The ratio of tau to Aβ also showed some weak correlations with atrophic rates in the combined group (critical p = 0.0004 in the temporal lobes and 0.001 in the whole brain). In the common sample, clinical correlations were compared with the results from CSF biomarkers. Baseline ADAS-cog and CDR-SB rates of decline were more strongly correlated with structural brain atrophy, as indicated by higher CDF curves and higher critical p values, with significant correlations also found in the separate diagnostic groups. Again, the effect sizes are substantially boosted by focusing on a temporal lobe region of interest, rather than including all the voxels in the brain; this is clearly evident as the curves on the right of each plot tend to rise more steeply at the original and intersect the FDR reference line ($y = 20x$) at a higher

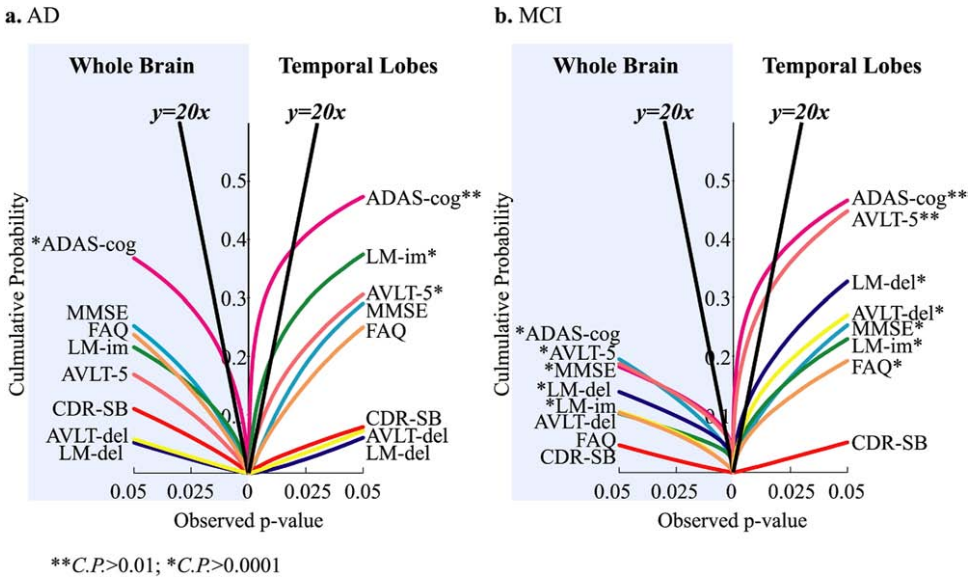

Fig. 3. Whole brain and temporal lobe atrophic rates are correlated with baseline clinical measures in Alzheimer's disease (AD) (a) and mild cognitive impairment (MCI) (b) groups. Significant correlations are marked with a critical p value greater than 0.01 or 0.0001. Interestingly, the Alzheimer's Disease Assessment Scale-cognitive subscale (ADAS-cog), perhaps the most widely used cognitive measure in clinical trials, was most strongly correlated at baseline with future atrophic rates, in both AD and MCI groups. Again, the cumulative distribution functions (CDF) curves for the temporal lobe data tend to rise more sharply at the origin, compared with curves computed from all the voxels in the brain. This is visually evident when comparing curves of the same color on each side of the plot. AVLT, Rey Auditory Verbal Learning Test; AVLT-5, AVLT conducted immediately after each of the 5 learning trials; AVLT-del, AVLT conducted after a 30-minute delay; CDR-SB, Sum-of-boxes Clinical Dementia Rating; FAQ, Functional Assessment Questionnaire; LM, Logical Memory; LM-del, LM test conducted after a 30-minute delay; LM-im, LM test conducted immediately after information was read to the subject; MMSE, Mini Mental State Examination; C.P., critical p value.

intersection point, whose x-value denotes the highest p value threshold that can be applied to the statistical maps while preserving the expected false discovery rate at the conventional level of 5%.

3.4. Temporal lobe atrophy rates linked to AD risk genes

Carriers of the ϵ4 allele of the ApoE (apolipoprotein E) gene, a commonly carried risk gene for late-onset AD (Roses and Saunders, 1994; Saunders et al., 1993), showed faster atrophic rates in the temporal lobes overall. Associations were weak but significant within each diagnostic group individually only inside the temporal lobes, but strong when all groups were combined (Fig. 6). The newly discovered risk allele (rs-10845840, which codes for GRIN2b, a glutamate receptor subunit; Stein et al., 2010) was associated with atrophic rates in the combined group, but more weakly than ApoE (Fig. 6; higher curves denote stronger effects). When ApoE4 was added to the statistical model that estimated the age and sex effects on the rates of atrophy, the sex effect turned out to be stronger (AD: critical $p = 0.001$; MCI: 0.02; CTL: not significant; ALL: 0.02) but the age effect was slightly attenuated (AD: not significant; MCI: critical $p = 0.007$; CTL: 0.0008; ALL: 0.01) inside the temporal lobes.

When expanding the search region to the whole brain, the presence of the ApoE4 risk allele was no longer associated with higher atrophic rates in individual diagnostic groups, but the effect remained significant in the combined group.

3.5. Faster temporal lobe atrophy in converters to AD within 1 year

MCI subjects who converted to AD within a year (13% of the total MCI group) showed faster atrophic rates than non-converters, as seen in the contrast map and the significance map (Fig. 7). Converters, on average, displayed 2%–3% faster atrophic rates than non-converters in the temporal lobes. A similar test in the whole brain did not reach statistical significance (critical p = not significant).

3.6. Correlations between atrophic rates and other risk factors

We evaluated correlations between atrophic rates and histories of cardiovascular, endocrine-metabolic, gastrointestinal disorders, alcohol abuse, drug abuse, and smoking. A medical history of drug abuse was weakly associated with a faster rate of tissue atrophy (critical $p = 0.0001$) in the AD group only, while the other factors had no detectable effect.

3.7. Using covariates to boost power in clinical trials

Given the age and sex effects in atrophic rates, we broke down the MCI groups into 6 age- and sex-divided subgroups. The n80s (sample size estimates) and 95% confidence intervals are shown in Table 1. In this table, lower

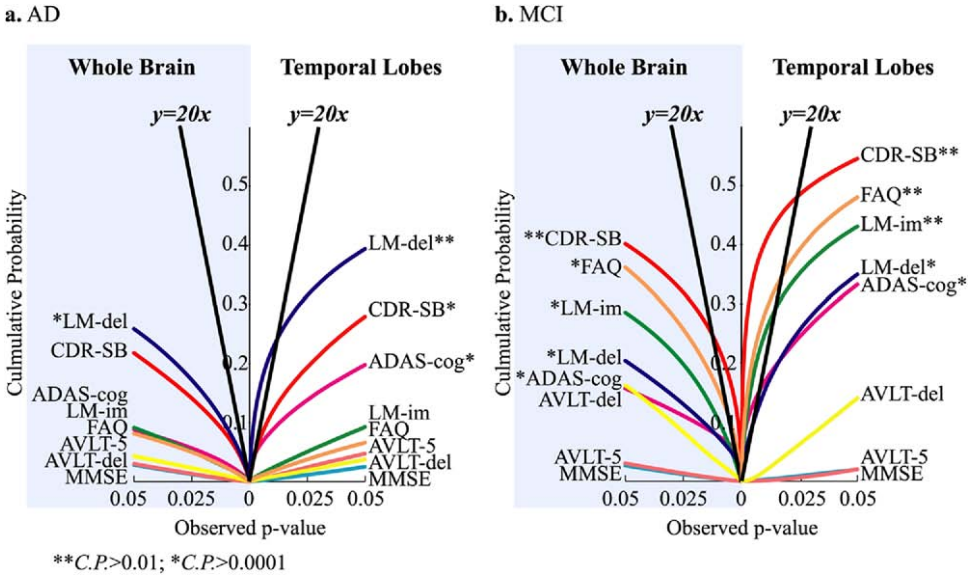

Fig. 4. Whole brain and temporal lobe atrophic rates correlated with rates of clinical decline, for various different clinical measures, in Alzheimer's disease (AD) (a) and mild cognitive impairment (MCI) (b) groups separately. Significant correlations are marked with critical $p > 0.01$ or > 0.0001. Sum-of-boxes Clinical Dementia Rating (CDR-SB) is the measure examined here whose change over time was the most highly correlated with atrophic rates in MCI. Comparison of curves of the same color on either side of the y axis shows that, in general, the analyses of the temporal lobe voxels give higher effect sizes (steeper cumulative distribution functions [CDFs] than those that include all the voxels in the brain. AVLT, Rey Auditory Verbal Learning Test; AVLT-5, AVLT conducted immediately after each of the 5 learning trials; AVLT-del, AVLT conducted after a 30-minute delay; CDR-SB, Sum-of-boxes Clinical Dementia Rating; FAQ, Functional Assessment Questionnaire; LM, Logical Memory; LM-del, LM test conducted after a 30-minute delay; LM-im, LM test conducted immediately after information was read to the subject; MMSE, Mini Mental State Examination; C.P., critical p value.

numbers are considered better as they imply that smaller sample sizes would be required to detect a 25% change in the rate of disease progress, measured by a specific AD biomarker, in response to a potentially disease-modifying drug. Younger men gave smaller n80s than older men, as expected from the age effects in MCI, where younger MCI subjects showed faster atrophy. For the sample size to be smaller, the atrophic rate may be higher and/or its standard deviation smaller. Women aged 60–70 or 70–80 had smaller n80s than men at similar ages. This is also consistent with the earlier finding that women had marginally faster atrophic rates in MCI (by ~0.5%–1.5% per year locally). In other words, trials focusing on younger subjects, or with subanalyses focusing on women versus men, would be better powered with these measures.

3.8. n80 for the CSF biomarkers

To compare structural MRI versus CSF biomarkers, we computed the n80s based on 1-year changes in CSF biomarker levels. Given their poorer reproducibility than MRI, the n80s were much larger than those from neuroimaging measures (Table 2). Although clearly not their intended use, tens of thousands to millions of subjects would need to be recruited to detect a potential drug effect using CSF biomarkers as surrogate markers measuring the rate of disease progression.

4. Discussion

In one of the largest ADNI 1-year follow-up studies, we applied TBM to map the rates of atrophy throughout the brain. Atrophic rates were shown to be correlated with some demographic factors (age and sex), but not education or BMI (although BMI has been associated with baseline levels of atrophy in an independent sample of normal subjects (Raji, et al., 2010). Atrophic rates were also associated with CSF biomarker levels (Aβ, tau, p-tau, tau/Aβ), cognitive performance, behavioral assessments, and risk genes (ApoE, GRIN2b).

In this study, greatest atrophy was primarily localized to the temporal lobes and several broadly distributed gray and white matter regions, and was evidenced by ventricular expansions (Fig. 2). This pattern of localization of atrophy agrees with many prior reports using voxel-based morphometry, tensor-based morphometry, and cortical thickness maps (Baron et al., 2001; Chetelat et al., 2002; Frisoni et al., 2009; Karas et al., 2004; Pievani et al., 2009; Scahill et al., 2002; Smith, 2002; Smith and Jobst, 1996; Whitwell et al., 2007), based on cross-sectional data or smaller longitudinal studies.

This study was preceded by a smaller pilot study (20 AD, 40 MCI, 40 CTL) with a similar design, in which temporal lobe atrophy rates were correlated with clinical measures and biomarkers (Leow et al., 2009). The current study substantially extended the earlier study by expanding the

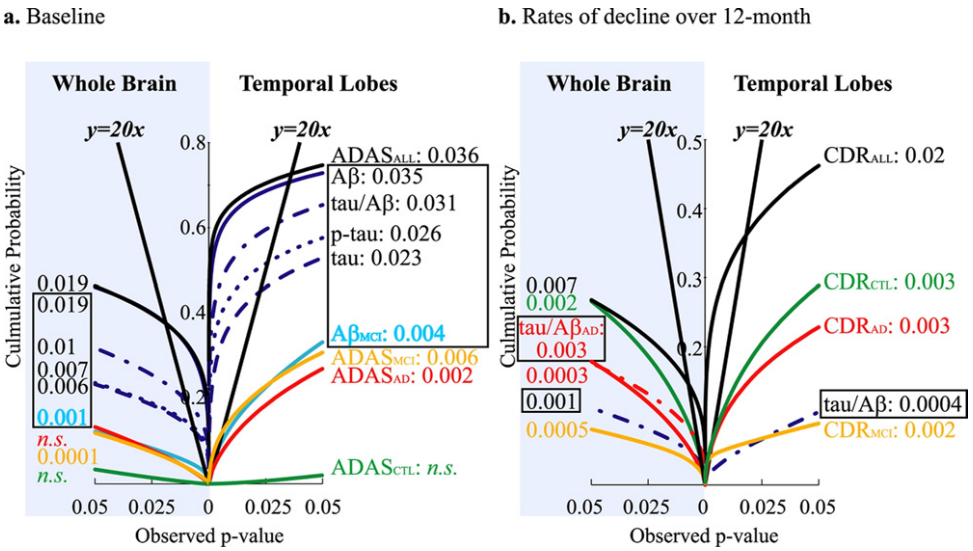

Fig. 5. Correlations between atrophic rates and cerebrospinal fluid (CSF) biomarker levels (biomarker and clinical labels are with and without borders, respectively). Whole brain and temporal lobe atrophic rates were correlated with biomarker levels in the following rank order, from strongest to weakest correlations: beta-amyloid peptides (Aβ), tau/Aβ, phosphorylated tau proteins (p-tau), and tau, in CSF at baseline, in the combined group of all control ($_{ALL}$), mild cognitive impairment (MCI; $_{MCI}$), and Alzheimer's disease (AD; $_{AD}$) subjects (blue cumulative distribution function [CDF] curves) (a). CSF Aβ levels were weakly correlated with atrophic rates (critical $p = 0.004$ in the temporal lobes and 0.001 in the whole brain) in the MCI group (cyan curves) (b). The amount of change in tau/Aβ over 12 months was weakly linked to brain atrophic rates. Clinical correlations, computed in the common dataset, were compared with the results from CSF biomarkers. In this common subsample, baseline Alzheimer's Disease Assessment Scale-cognitive subscale (ADAS-cog) (a) and Sum-of-boxes Clinical Dementia Rating (CDR-SB) (labeled as CDR) rates of decline (b) are more strongly correlated with structural brain atrophy, as indicated by higher CDF curves and critical p values compared with CSF biomarker correlations. All. other correlations, with baseline and longitudinal measures of CSF biomarkers, were not significant (not shown in the graph). C.P., critical p value; *n.s.*, not significant.

search region to the whole brain, and by investigating age and sex effects as well as correlations with many newly added biomarkers and risk factors in a sample size almost 7 times larger. We confirmed earlier findings that temporal lobe atrophy rates were faster in MCI converters than non-converters, and were correlated with baseline CSF biomarker levels (Aβ, tau, p-tau, tau/Aβ) in the combined group, with baseline LM-del in MCI, and with changes of CDR-SB and LM-im in MCI; however, rate of atrophy, in the current study, was not shown to correlate with baseline level of p-tau, change in MMSE, and change in AVLT-del in MCI. The discrepancy might be due to the sample composition (although sample selection was unbiased) but is more likely due to the sample size difference, which is 7 times larger here. Additionally, we identified significant age and sex differences in atrophic rates; temporal lobe atrophy rates correlated with Aβ in MCI, baseline ADAS-cog, LM-im, and AVLT-5 in AD, baseline ADAS-cog, AVLT-5, AVLT-del, LM-im, FAQ, and MMSE in MCI, changes in LM-del, ADAS-cog, and CDR-SB in AD, and changes in FAQ, ADAS-cog, and LM-del in MCI. In the current study, we were also able to detect the associations between common variants in the ApoE and GRIN2b genes and brain atrophic rates; we also explored the implications of drug trial enrichment by performing subanalyses based on this information.

4.1. Age and sex effects

4.1.1. Age effects

The age effects on atrophic rates in our study are based on comparing atrophic rates in individuals, which is not to be confused with mapping disease acceleration or deceleration within individual subjects scanned more than twice (Sluimer et al., 2009). A recent non-ADNI study of individuals with 3 or more serial MRI scans (46 amnestic MCI subjects who later converted to AD, 46 healthy controls, and 23 stable MCI subjects) found that the rates of atrophy do tend to accelerate as individuals progress from amnestic MCI to typical late-onset AD; and the rates of atrophy were greater in younger than older MCI subjects (Jack et al., 2008c). Our study, in a much larger sample of 684 ADNI subjects (114 AD, 338 MCI, and 202 CTL), confirmed the trend for faster degeneration in younger amnestic MCI subjects versus older subjects. The most plausible explanation is that younger MCI subjects have a more biologically aggressive disease course than older subjects (Jack et al., 2008c). There is substantial clinical and neuroimaging evidence that early-onset AD (onset before age 65 and typically in the 40s and 50s) generally represents a more aggressive form of disease than late-onset AD (onset after age 65) (Frisoni et al., 2007). A second possibility is that younger MCI subjects may have a larger cognitive reserve than older subjects; under this theory, young people may

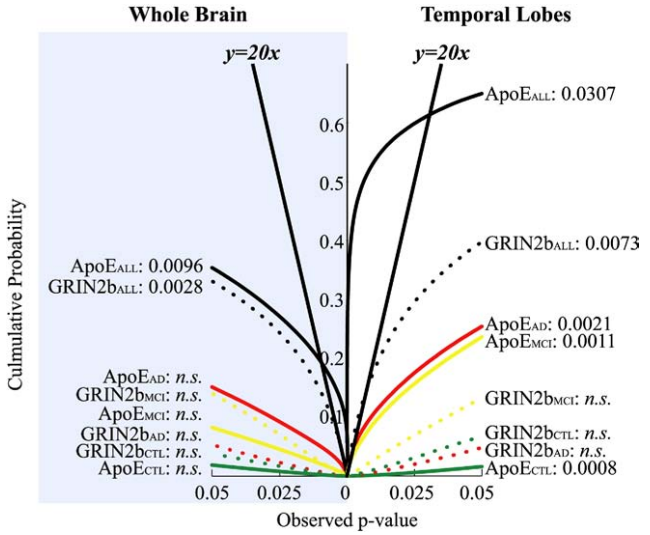

Fig. 6. Genetic influences on brain atrophy. The presence of the ApoE4 (marked by solid lines) and the GRIN2b risk gene (also known as single nucleotide polymorphism [SNP] rs-10845840; dotted lines; Stein et al., 2010) were associated with faster rates of atrophy in the temporal lobes, with ApoE4 showing a greater statistical influence than GRIN2b, indicated by the rank order of the cumulative distribution functions (CDFs) and by the false discovery rate (FDR) critical p values. When expanding the search region to the whole brain, the presence of the ApoE4 risk allele was no longer associated with higher atrophic rates in individual diagnostic groups, but the effect remained significant in the combined group. Risk genes were coded as 0, 1, and 2 for 0, 1 risk allele, and 2 adverse alleles, respectively; association tests assumed an additive model of gene action. Critical p values are shown for each test. AD, Alzheimer's disease; MCI, mild cognitive impairment; CTL, healthy elderly controls; ALL, all subjects including AD, MCI, and CTL; *n.s.*, not significant.

have greater ability to compensate for the brain deficits so that symptoms may not be evident until brain atrophy has progressed to a greater degree, and is proceeding faster (see, e.g., Mortimer et al., 2005; but see also Christensen et al., 2007 for an opposing view). Finally, some very old subjects were assessed (80–90 years of age), so one has to keep in mind the possibility of a selection bias. Very old people in the study might tend to be more well (well enough to participate in a neuroimaging study requiring multiple follow-ups), and have lower atrophic rates; even though when those same people were younger (long before ADNI) they may have had even slower atrophy rates. In other words, early mortality may prevent people from enrolling in ADNI if they die earlier due to very fast atrophy, so the oldest subjects in ADNI, as a survivor effect, may have slower atrophic rates for this reason. This attrition effect could explain the paradoxical "adverse" effect of young age in a cross-sectional study (faster atrophy in younger people), even when people's atrophic rates may speed up as the disease progresses (within an individual); this has been demonstrated in early-onset AD (Chan et al., 2003; Ridha et al., 2006) and late-onset AD (Jack et al., 2008c). In a normal aging study, Scahill et al. (2003) found evidence that atrophic rates accelerated with increasing age; our study also showed a small age effect in the control group, with a similar direction of correlation.

4.1.2. Sex effects

We provided the first structural MRI evidence, to our knowledge, of sexual dimorphism in atrophic rates, although several studies have found worse cognitive and behavioral deficits in women versus men with AD. Most early MRI studies failed to detect a sex difference in atrophic rates, but were limited by small sample sizes and limited statistical power. Sex differences in brain structure are found naturally and well studied (see, e.g., Brun et al., 2009 for a TBM study) but sex differences in the rates of brain change over time are less commonly reported, except in studies of childhood brain development where they occur around puberty (Giedd et al., 1999). Why atrophic rate was faster in women is not clear. Numerous demographic studies provide evidence for a "male-female health-survival paradox". According to this, older men are generally in better health and are less limited in their daily activities than women of the same age, but mortality rates are higher in men than women at all ages (Christensen, 2008). Genetic variation in the sex chromosomes may contribute to sex differences in the incidence of some comorbid disorders. Men may have earlier and higher incidence of hypertension and cardiovascular diseases (high mortality risk diseases) while women suffer more from migraine, arthritis, and musculoskeletal diseases (low mortality risk diseases) (Macintyre et al., 1996); this may be related to the cohort effect discussed earlier. Sex hormones may also influence the expression of genes that affect lifespan and longevity (Tower, 2006; Tower and Arbeitman, 2009).

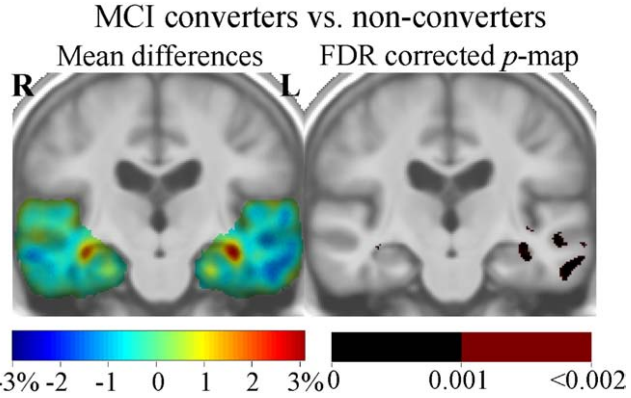

Fig. 7. Mild cognitive impairment (MCI) converters showed faster rates of brain atrophy in temporal lobes than MCI non-converters. The mean difference map shows regions where atrophy rates are faster in converters than non-converters (left panel; blue colors: 3% faster). Red colors show regions where ventricular expansion is faster in converters than nonconverters. The right panel shows the false discovery rate (FDR) corrected p maps displaying regions with significant difference overall (critical $p = 0.002$).

Table 1
The n80s for groups of MCI subjects subdivided by age and sex, and in the combined group with all MCI subjects included

	60–70 years	70–80 years	80–90 years
Women	46 [26,102]	55 [40, 88]	117 [70,233]
Men	68 [47,108]	96 [69,147]	117 [83,182]
Combined	90 [75, 110]		

Sub-analyses focusing on women or younger subjects led to smaller sample size estimates (or, equivalently, greater power to detect a disease slowing effect in a given sample size). The numerical summaries, used for computing n80s, were generated within a statistically predefined ROI inside the gray matter of the entire brain, providing an overall estimate of the gray matter atrophic rate for each individual.

4.1.3. Baseline differences

We identified significant age and sex differences in baseline measures of brain atrophy, within each group independently and in the combined group. These baseline effects may reflect a combination of (1) the cumulative influence of age and sex throughout life, and (2) naturally occurring sex differences in brain structure, as different structures tend to occupy different proportions of the total brain volume in men versus women (i.e., allometry; Brun et al., 2009). Lower education levels are also linked to a higher risk of developing AD and faster rate of progression when compared with more highly educated people (Ngandu et al., 2007; Scarmeas et al., 2006). Higher BMI, an index of obesity, is associated with greater brain atrophy in elderly normal subjects (Raji, et al., 2010). We therefore added education and BMI to the statistical models of age and sex, but the conclusions remained the same even after adjusting for these additional factors. BMI was associated with baseline atrophy but not with atrophic rates.

4.2. Structural MRI, clinical, and CSF biomarkers

Different biomarkers provide complementary information at different stages of AD (Jack et al., 2008b; Jagust et al., 2009). In particular, structural MRI measures tend to correlate better with cognitive test scores than with CSF biomarker levels. This may be because (1) CSF biomarker changes tend to precede the gross anatomical changes on MRI, and (2) because CSF measures are primarily intended to help with diagnosis rather than resolve subtle changes over time within diagnostic categories. We note that CSF measures were not used to assist diagnosis in the ADNI study. However, at least part of the difference in statistical power is due to the different sample sizes of subjects who had available cognitive measures versus CSF biomarker measures. We tested a common set of subjects who had both cognitive and CSF measures (Fig. 5). By reducing the full sample (n = 684 at baseline and n = 660 with 1-year follow-up) to the common set (n = 363 at baseline and n = 251 with 1-year follow-up), the clinical correlations all became weaker; however, their statistical effects remained higher than those of CSF biomarkers — for example, there were significant correlations even within the separate diagnostic groups, while only a couple of CSF biomarkers (baseline level of Aβ in MCI and rate of tau/Aβ decline in AD) survived statistical testing within the separate diagnostic groups.

4.3. AD risk genes

ApoE4 is a well-known AD risk gene (Corder et al., 1993, Roses, 1996; Roses and Saunders, 1994, Roses et al., 1995, Saunders et al., 1993), and in our earlier cross-sectional study of 676 ADNI subjects, ApoE2 (the "protective" allele) was associated with reduced CSF volume (an index of lesser brain atrophy) and ApoE4 was associated with greater temporal lobe atrophy (Hua et al., 2008b). In this longitudinal analysis, ApoE4 and GRIN2b were linked to faster rates of temporal lobe atrophy, in a dose-dependent fashion. GRIN2b is a newly identified risk SNP that predicts temporal lobe volumes in ADNI at baseline (Stein et al., 2010), but its association with AD is not as strong as ApoE, so requires replication. As well as its use for measuring disease progression, structural MRI measures can also be used to identify genes that influence brain volumes in genome-wide association studies (GWAS) (Joyner et al., 2009; Potkin et al., 2009; Stein et al., 2010).

4.4. Statistical analyses

We applied stratified analyses and ran separate regressions independently in each diagnostic group, to ensure that the observed statistical effects were not driven by diagnosis. Alternatively, the analysis could be carried out by pooling all subjects, by applying indicator variables to encode diagnostic groups and interaction terms to quantify inter-group differences on the main effects. However, this increases the computational burden, and each analysis already involves ~2,000,000 correlations. Because of the very large number of possible interactions, and the likelihood of not being able to fit them all stably, we did not test for interactions between diagnostic groups and predictor variables. We also did not attempt to quantify inter-group differences in the main ef-

Table 2
The sample sizes (n80s) for AD and MCI using CSF biomarkers versus MRI measures of whole-brain gray matter atrophy and temporal lobe atrophy

	AD (n = 50)	MCI (n = 122)
CSF biomarkers		
A$\beta_{1\text{-}42}$	5,721,531	75,816
t-tau	81,292	19,098
t-tau/A$\beta_{1\text{-}42}$	66,293	533,091
MRI measures		
Gray matter atrophy	43	86
Temporal lobe atrophy	43	82

The numerical summaries of MRI imaging measures were generated within a statistically predefined ROI with the gray matter of the entire brain and in the temporal lobes, providing a measure of the overall gray matter atrophic rate and temporal lobe atrophic rates, respectively. AD, Alzheimer's disease; MCI, mild cognitive impairment; MRI, magnetic resonance imaging; CSF, cerebrospinal fluid.

fects, which requires a second order analysis and has still greater statistical power requirements. Instead, we treated the 3 diagnostic groups independently, merely to ensure that the observed statistical effects were not driven by diagnosis.

In all analyses, we first ran correlations in the separate clinical groups, and then we ran another correlation in the combined group, where appropriate. This is the most agnostic approach as it allows the correlations to differ, in principle, in the different diagnostic categories, avoiding the risk that the detected correlations may be shadowing diagnosis. We did not perform correlations with clinical measures in the combined group. As clinical measures are used to determine diagnosis, a correlation in the combined group will be significant by construction. The CSF biomarkers, however, were not used to define diagnosis so it is reasonable to correlate them with levels of atrophy across the combined group. Even so, correlations detected in the combined group may not even apply within some of the groups, either indicating a lack of association or, more likely, limited power to track subtle disease progression within the reduced samples of subjects in individual diagnostic groups. This effect likely explains the lack of correlations with CSF biomarkers within groups. The correlations between CSF biomarkers and MRI changes tend to break down as the disease progresses, as changes in CSF biomarker levels may primarily occur prior to the MRI changes. A similar pattern has been noted in studies of amyloid PET (Braskie et al., 2008), where cortical thinning may not correlate with amyloid deposition if the 2 processes occur or saturate at different times. In a recent study using serial imaging, the rate of neurodegeneration was shown to associate with clinical symptoms but dissociate from amyloid deposition measured by $^{[11]}$C Pittsburgh compound B (PIB) positron emission tomography (Jack et al., 2009).

We used categorical variables or indicator variables to encode binary predictors, such as sex, medical history, and conversion to AD, each of these variables only has 2 distinct classes, i.e., male versus female, those with or without a medical history, and converters versus non-converters. If a simple linear regression only includes a 2-class categorical variable as the independent variable, the regression acts as a 2-sample Student *t* test. An added benefit of using regressions over *t* tests is that regression allowed us to control for effects of several covariates simultaneously. For example, by fitting both age and sex in the regression model, the sex effect was controlled for when assessing any age effects on atrophic rates.

4.5. Choices of search region

The results in the whole brain ROI are generally consistent with those derived from the temporal lobes, but are weaker in statistical power. This is expected as brain degeneration is not uniformly distributed across the brain, nor does it progress uniformly. The volume loss pattern from mild to moderate AD spreads over time from temporal and limbic cortices into frontal and occipital brain regions, largely sparing primary sensorimotor cortices (Braak and Braak, 1991; Thompson et al., 2003). One advantage of focusing on the temporal lobes is the improved statistical power by restricting the search region to the area most affected in MCI and early AD. In examining genes influencing brain atrophy (Fig. 6) and comparing differences between groups of MCI converters and non-converters (Fig. 7), the statistical effects were only significant in the temporal lobes —which makes sense as these are the regions with greatest pathologic burden in early AD. The inclusion of many voxels with much slower atrophic rates and with lower effect sizes tends to inflate the number of voxels assessed to the point where no FDR-controlling threshold can be found. Nevertheless, it is also important to examine the results across the entire brain to better understand factors influencing brain atrophy in normal aging and AD.

4.6. Conclusions and limitations

Our study is 1 of many that support the use of structural MRI for providing valid surrogate markers in clinical drug trials. MRI is also useful for detecting factors that affect structural changes in anatomical regions involved in AD. CSF biomarkers, despite their value for early diagnosis, might not be so effective for tracking disease progression over time or even for evaluating therapeutic interventions in MCI and AD. For example, their n80s — measures of sample size requirements to detect a fixed percent reduction in the rate of progression — are 1000–10,000 times larger than those from structural MRI (Table 2).

TBM-derived maps of atrophic rates, coupled with voxel-based statistics, offer an easy-to-implement process to investigate factors that exert negative or positive influences on aging and AD. Full 3-dimensional maps are used in these correlations, as opposed to only 1 biomarker measure per individual. This type of map-based method may offer more information and spatial detail on the profile of effects, and may offer better statistical power if effect sizes are not constant across the brain.

Each AD biomarker, derived from structural MRI, clinical, or CSF measures, can be used independently to evaluate drug treatment effects, providing a surrogate outcome measure to track the rate of disease progress. As a result of using different biomarkers, the sample size estimates (n80) should be interpreted with care. For example, a 25% reduction in the atrophic rate (measured by MRI) may have a different functional significance for a patient than a 25% reduction in the rate of decline for clinical or cognitive test scores; similarly, it may also have a different biological significance than a 25% reduction in the rate of change in CSF biomarkers. For example, there may be important and relevant biological events that do not have an immediate imaging correlate. Future efforts will focus on combining multiple biomarkers that measure different aspects of disease progress to reduce the sample size even further.

This study has some limitations. The age and sex effects on atrophic rates, which were still significant here after controlling for education, BMI, and ApoE4, need to be replicated in future independent studies. A more complete dataset from a large number of subjects with MRI, PIB-PET, [18F] fluorodeoxyglucose (FDG)-PET, diffusion tensor imaging (DTI), resting-state functional MRI, and arterial spin labeling is now being collected to explore the complementary value of each of these neuroimaging markers. Future longitudinal ADNI studies will make use of more than 2 serial scans, allowing acceleration hypotheses regarding age effects to be tested in the same subjects. More advanced statistical designs, such as random effects or mixed effects models, may then be used to estimate intra-subject variance and group effects with repeated measures (Fitzmaurice et al., 2004; Frost et al., 2004; Schuff et al., 2009).

Disclosure statement

The authors have no potential financial or personal conflicts of interest including relationships with other people or organization within 3 years of beginning the work submitted that could inappropriately influence their work.

The study was conducted according to the Good Clinical Practice guidelines, the Declaration of Helsinki, US 21 CFR Part 50-Protection of Human Subjects, and Part 56-Institutional Review Boards. Written informed consent was obtained from all participants.

Acknowledgments

Data collection and sharing for this project was funded by the Alzheimer's Disease Neuroimaging Initiative (ADNI) (National Institutes of Health Grant U01 AG024904). ADNI is funded by the National Institute on Aging, the National Institute of Biomedical Imaging and Bioengineering, and through generous contributions from the following: Abbott, AstraZeneca AB, Bayer Schering Pharma AG, Bristol-Myers Squibb, Eisai Global Clinical Development, Elan Corporation, Genentech, GE Healthcare, GlaxoSmithKline, Innogenetics, Johnson and Johnson, Eli Lilly and Co., Medpace, Inc., Merck and Co., Inc., Novartis AG, Pfizer Inc, F. Hoffman-La Roche, Schering-Plough, Synarc, Inc., and Wyeth, as well as nonprofit partners the Alzheimer's Association and Alzheimer's Drug Discovery Foundation, with participation from the US Food and Drug Administration. Private sector contributions to ADNI are facilitated by the Foundation for the National Institutes of Health (www.fnih.org). The grantee organization is the Northern California Institute for Research and Education, and the study is coordinated by the Alzheimer's Disease Cooperative Study at the University of California, San Diego. ADNI data are disseminated by the Laboratory of Neuro Imaging at the University of California, Los Angeles.

This research was also supported by NIH grants P30 AG010129, K01 AG030514, and the Dana Foundation. Algorithm development and image analysis for this study was funded by grants to PT from the NIBIB (R01 EB007813, R01 EB008281, R01 EB008432), NICHD (R01 HD050735), and NIA (R01 AG020098), and National Institutes of Health through the NIH Roadmap for Medical Research Grants U54-RR021813 (CCB) (to AWT and PT). Author contributions were as follows: XH, DH, SL, AT, and PT performed the image analyses; CJ and MW contributed substantially to the image and data acquisition, study design, quality control, calibration and preprocessing, databasing and image analysis. We thank Anders Dale for his contributions to the image preprocessing and the ADNI project.

Data used in the preparation of this article were obtained from the Alzheimer's Disease Neuroimaging Initiative (ADNI) database (www.loni.ucla.edu/ADNI). As such, the investigators within the ADNI contributed to the design and implementation of ADNI and/or provided data but did not participate in analysis or writing of this report. A complete list of ADNI investigators is available at: www.loni.ucla.edu/ADNI/Collaboration/ADNI_Manuscript_Citations.pdf.

References

Consensus report, 1998, of the Working Group on: ″Molecular and Biochemical Markers of Alzheimer's Disease″. The Ronald and Nancy Reagan Research Institute of the Alzheimer's Association and the National Institute on Aging Working Group [erratum in: 1998;19(3): 28]. Neurobiol. Aging 19, 109-116.

Apostolova, L.G., Dutton, R.A., Dinov, I.D., Hayashi, K.M., Toga, A.W., Cummings, J.L., Thompson, P.M., 2006. Conversion of mild cognitive impairment to Alzheimer disease predicted by hippocampal atrophy maps. Arch. Neurol. 63, 693–699.

Ashburner, J., Friston, K.J., 2003. Morphometry. Human Brain Function. San Diego: Academic Press.

Bai, F., Zhang, Z., Watson, D.R., Yu, H., Shi, Y., Zhu, W., Wang, L., Yuan, Y., Qian, Y., 2009. Absent gender differences of hippocampal atrophy in amnestic type mild cognitive impairment. Neurosci. Lett. 450, 85–89.

Baron, J.C., Chetelat, G., Desgranges, B., Perchey, G., Landeau, B., de la Sayette, V., Eustache, F., 2001. In vivo mapping of gray matter loss with voxel-based morphometry in mild Alzheimer's disease. Neuroimage 14, 298–309.

Benjamini, Y., Hochberg, Y., 1995. Controlling the false discovery rate: a practical and powerful approach to multiple testing. J. R. Stat. Soc. B 57, 289–300.

Berg, L., 1988. Clinical Dementia Rating (CDR). Psychopharmacol. Bull. 24, 637–639.

Braak, H., Braak, E., 1991. Neuropathological stageing of Alzheimer-related changes. Acta Neuropathol. (Berl.) 82, 239–259.

Braskie, M.N., Klunder, A.D., Hayashi, K.M., Protas, H., Kepe, V., Miller, K.J., Huang, S.C., Barrio, J.R., Ercoli, L.M., Siddarth, P., Satyamurthy, N., Liu, J., Toga, A.W., Bookheimer, S.Y., Small, G.W., Thompson, P.M., 2008. Plaque and tangle imaging and cognition in normal aging and Alzheimer's disease. Neurobiol. Aging, in press. Epub ahead of print: http://www.ncbi.nlm.nih.gov/pubmed/19004525?dopt=Citation.

Brun, C.C., Lepore, N., Luders, E., Chou, Y.Y., Madsen, S.K., Toga, A.W., Thompson, P.M., 2009. Sex differences in brain structure in auditory and cingulate regions. Neuroreport 20, 930–935.

Carmichael, O.T., Thompson, P.M., Dutton, R.A., Lu, A., Lee, S.E., Lee, J.Y., Kuller, L.H., Lopez, O.L., Aizenstein, H.J., Meltzer, C.C., Liu, Y., Toga, A.W., Becker, J.T., 2006. Mapping ventricular changes related to dementia and mild cognitive impairment in a large community-based cohort. IEEE ISBI, 315–318.

Chan, D., Janssen, J.C., Whitwell, J.L., Watt, H.C., Jenkins, R., Frost, C., Rossor, M.N., Fox, N.C., 2003. Change in rates of cerebral atrophy over time in early-onset Alzheimer's disease: longitudinal MRI study. Lancet 362, 1121–1122.

Chen, K., Reschke, C., Lee, W., Napatkamon, A., Liu, X., Bandy, D., Langbaum, J., Alexander, G.E., Foster, N.L., Koeppe, R.A., Jagust, W.J., Weiner, M.W., Reiman, E.M., 2009. Cross-sectional and longitudinal analyses of fluorodeoxyglucose positron emission tomography images from the Alzheimer's disease neuroimaging initiative. ADNI Data Presentations Meeting, Seattle, WA. http://www.adni-info.org/Pdfs/11_reiman_adni.pdf).

Chetelat, G., Desgranges, B., De La Sayette, V., Viader, F., Eustache, F., Baron, J.C., 2002. Mapping gray matter loss with voxel-based morphometry in mild cognitive impairment. Neuroreport 13, 1939–1943.

Chetelat, G., Baron, J.C., 2003. Early diagnosis of Alzheimer's disease: contribution of structural neuroimaging. Neuroimage 18, 525–541.

Chetelat, G., Fouquet, M., Kalpouzos, G., Denghien, I., De la Sayette, V., Viader, F., Mezenge, F., Landeau, B., Baron, J.C., Eustache, F., Desgranges, B., 2008. Three-dimensional surface mapping of hippocampal atrophy progression from MCI to AD and over normal aging as assessed using voxel-based morphometry. Neuropsychologia 46, 1721–1731.

Chou, Y.Y., Leporé, N., Avedissian, C., Madsen, S.K., Hua, X., Jack Jr, C.R., Weiner, M.W., Toga, A.W., Thompson, P.M., 2009a. Mapping ventricular expansion and its clinical correlates in Alzheimer's disease and mild cognitive impairment using multi-atlas fluid image alignment. Proceedings of SPIE Medical Imaging 2009, SPIE Paper Number 7259-111, February 9, 2009.

Chou, Y.Y., Lepore, N., Avedissian, C., Madsen, S.K., Parikshak, N., Hua, X., Shaw, L.M., Trojanowski, J.Q., Weiner, M.W., Toga, A.W., Thompson, P.M., 2009b. Mapping correlations between ventricular expansion and CSF amyloid and tau biomarkers in 240 subjects with Alzheimer's disease, mild cognitive impairment and elderly controls. Neuroimage 46, 394–410.

Chou, Y.Y., Lepore, N., de Zubicaray, G.I., Carmichael, O.T., Becker, J.T., Toga, A.W., Thompson, P.M., 2008. Automated ventricular mapping with multi-atlas fluid image alignment reveals genetic effects in Alzheimer's disease. Neuroimage 40, 615–630.

Christensen, H., Anstey, K.J., Parslow, R.A., Maller, J., Mackinnon, A., Sachdev, P., 2007. The brain reserve hypothesis, brain atrophy and aging. Gerontology 53, 82–95.

Christensen, K., 2008. Human biodemography: Some challenges and possibilities for aging research. Demographic Research 19, 1575–1586.

Chung, M.K., Worsley, K.J., Paus, T., Cherif, C., Collins, D.L., Giedd, J.N., Rapoport, J.L., Evans, A.C., 2001. A unified statistical approach to deformation-based morphometry. Neuroimage 14, 595–606.

Clark, C.M., Davatzikos, C., Borthakur, A., Newberg, A., Leight, S., Lee, V.M., Trojanowski, J.Q., 2008. Biomarkers for early detection of Alzheimer pathology. Neurosignals 16, 11–18.

Clark, C.M., Xie, S., Chittams, J., Ewbank, D., Peskind, E., Galasko, D., Morris, J.C., McKeel, D.W., Jr., Farlow, M., Weitlauf, S.L., Quinn, J., Kaye, J., Knopman, D., Arai, H., Doody, R.S., DeCarli, C., Leight, S., Lee, V.M., Trojanowski, J.Q., 2003. Cerebrospinal fluid tau and beta-amyloid: how well do these biomarkers reflect autopsy-confirmed dementia diagnoses? Arch. Neurol. 60, 1696–1702.

Clarkson, M.J., Ourselin, S., Nielsen, C., Leung, K.K., Barnes, J., Whitwell, J.L., Gunter, J.L., Hill, D.L., Weiner, M.W., Jack, C.R., Jr., Fox, N.C., 2009. Comparison of phantom and registration scaling corrections using the ADNI cohort. Neuroimage 47, 1506–1513.

Cockrell, J.R., Folstein, M.F., 1988. Mini-Mental State Examination (MMSE). Psychopharmacol. Bull. 24, 689–692.

Collins, D.L., Neelin, P., Peters, T.M., Evans, A.C., 1994. Automatic 3D intersubject registration of MR volumetric data in standardized Talairach space. J. Comput. Assist. Tomogr. 192–205.

Corder, E.H., Saunders, A.M., Strittmatter, W.J., Schmechel, D.E., Gaskell, P.C., Small, G.W., Roses, A.D., Haines, J.L., Pericak-Vance, M.A., 1993. Gene dose of apolipoprotein E type 4 allele and the risk of Alzheimer's disease in late onset families. Science 261, 921–923.

Davison, A.C., Hinkley, D.V., 1997. Bootstrap Methods and Their Application. Cambridge: Cambridge University Press.

de Leon, M.J., DeSanti, S., Zinkowski, R., Mehta, P.D., Pratico, D., Segal, S., Rusinek, H., Li, J., Tsui, W., Saint Louis, L.A., Clark, C.M., Tarshish, C., Li, Y., Lair, L., Javier, E., Rich, K., Lesbre, P., Mosconi, L., Reisberg, B., Sadowski, M., DeBernadis, J.F., Kerkman, D.J., Hampel, H., Wahlund, L.O., Davies, P., 2006. Longitudinal CSF and MRI biomarkers improve the diagnosis of mild cognitive impairment. Neurobiol. Aging 27, 394–401.

Devanand, D.P., Pradhaban, G., Liu, X., Khandji, A., De Santi, S., Segal, S., Rusinek, H., Pelton, G.H., Honig, L.S., Mayeux, R., Stern, Y., Tabert, M.H., de Leon, M.J., 2007. Hippocampal and entorhinal atrophy in mild cognitive impairment: prediction of Alzheimer disease. Neurology 68, 828–836.

Dodge, H.H., Shen, C., Pandav, R., DeKosky, S.T., Ganguli, M., 2003. Functional transitions and active life expectancy associated with Alzheimer disease. Arch. Neurol. 60, 253–259.

Du, A.T., Schuff, N., Amend, D., Laakso, M.P., Hsu, Y.Y., Jagust, W.J., Yaffe, K., Kramer, J.H., Reed, B., Norman, D., Chui, H.C., Weiner, M.W., 2001. Magnetic resonance imaging of the entorhinal cortex and hippocampus in mild cognitive impairment and Alzheimer's disease. J. Neurol. Neurosurg. Psychiatry 71, 441–447.

Efron, B., Tibshirani, R.J., 1993. An Introduction to the Bootstrap. Chapman & Hall, New York.

Evans, M.C., Barnes, J., Nielsen, C., Kim, L.G., Clegg, S.L., Blair, M., Leung, K.K., Douiri, A., Boyes, R.G., Ourselin, S., Fox, N.C., 2010. Volume changes in Alzheimer's disease and mild cognitive impairment: cognitive associations. Eur. Radiol. 20, 674–682.

Fitzmaurice, G.M., Laird, N.M., Ware, J.H., 2004. Applied Longitudinal Analysis. NJ: Wiley-Interscience.

Fleisher, A., Grundman, M., Jack, C.R., Jr., Petersen, R.C., Taylor, C., Kim, H.T., Schiller, D.H., Bagwell, V., Sencakova, D., Weiner, M.F., DeCarli, C., DeKosky, S.T., van Dyck, C.H., Thal, L.J., 2005. Sex, apolipoprotein E epsilon 4 status, and hippocampal volume in mild cognitive impairment. Arch. Neurol. 62, 953–957.

Folstein, M.F., Folstein, S.E., McHugh, P.R., 1975. "Mini-mental state". A practical method for grading the cognitive state of patients for the clinician. J. Psychiatr. Res. 12, 189–198.

Fox, N.C., Cousens, S., Scahill, R., Harvey, R.J., Rossor, M.N., 2000. Using serial registered brain magnetic resonance imaging to measure disease progression in Alzheimer disease: power calculations and estimates of sample size to detect treatment effects. Arch. Neurol. 57, 339–344.

Fox, N.C., Scahill, R.I., Crum, W.R., Rossor, M.N., 1999. Correlation between rates of brain atrophy and cognitive decline in AD. Neurology 52, 1687–1689.

Frank, R.A., Galasko, D., Hampel, H., Hardy, J., de Leon, M.J., Mehta, P.D., Rogers, J., Siemers, E., Trojanowski, J.Q., 2003. Biological markers for therapeutic trials in Alzheimer's disease. Proceedings of the biological markers working group; NIA initiative on neuroimaging in Alzheimer's disease. Neurobiol. Aging 24, 521–536.

Freeborough, P.A., Fox, N.C., 1998. Modeling brain deformations in Alzheimer disease by fluid registration of serial 3D MR images. J. Comput. Assist. Tomogr. 22, 838–843.

Frisoni, G.B., Laakso, M.P., Beltramello, A., Geroldi, C., Bianchetti, A., Soininen, H., Trabucchi, M., 1999. Hippocampal and entorhinal cortex atrophy in frontotemporal dementia and Alzheimer's disease. Neurology 52, 91–100.

Frisoni, G.B., Pievani, M., Testa, C., Sabattoli, F., Bresciani, L., Bonetti, M., Beltramello, A., Hayashi, K.M., Toga, A.W., Thompson, P.M., 2007. The topography of grey matter involvement in early and late onset Alzheimer's disease. Brain 130, 720–730.

Frisoni, G.B., Prestia, A., Rasser, P.E., Bonetti, M., Thompson, P.M., 2009. In vivo mapping of incremental cortical atrophy from incipient to overt Alzheimer's disease. J. Neurol. 256, 916–924.

Frisoni, G.B., Fox, N.C., Jack Jr., C.R., Scheltens, P., Thompson, P.M., 2010. The clinical use of structural MRI in Alzheimer disease. Nat. Rev. Neurol. 6, 1–11.

Frost, C., Kenward, M.G., Fox, N.C., 2004. The analysis of repeated 'direct' measures of change illustrated with an application in longitudinal imaging. Stat. Med. 23, 3275–3286.

Gao, S., Hendrie, H.C., Hall, K.S., Hui, S., 1998. The relationships between age, sex, and the incidence of dementia and Alzheimer disease: a meta-analysis. Arch. Gen. Psychiatry 55, 809–815.

Genovese, C.R., Lazar, N.A., Nichols, T., 2002. Thresholding of statistical maps in functional neuroimaging using the false discovery rate. Neuroimage 15, 870–878.

Giedd, J.N., Blumenthal, J., Jeffries, N.O., Castellanos, F.X., Liu, H., Zijdenbos, A., Paus, T., Evans, A.C., Rapoport, J.L. 1999. Brain development during childhood and adolescence: a longitudinal MRI study. Nat. Neurosci. 2, 861–863.

Grundman, M., Petersen, R.C., Ferris, S.H., Thomas, R.G., Aisen, P.S., Bennett, D.A., Foster, N.L., Jack, C.R., Jr., Galasko, D.R., Doody, R., Kaye, J., Sano, M., Mohs, R., Gauthier, S., Kim, H.T., Jin, S., Schultz, A.N., Schafer, K., Mulnard, R., van Dyck, C.H., Mintzer, J., Zamrini, E.Y., Cahn-Weiner, D., Thal, L.J., 2004. Mild cognitive impairment can be distinguished from Alzheimer disease and normal aging for clinical trials. Arch. Neurol. 61, 59–66.

Gunter, J., Bernstein, M., Borowski, B., Felmlee, J., Blezek, D., Mallozzi, R., 2006. Validation testing of the MRI calibration phantom for the Alzheimer's Disease Neuroimaging Initiative Study. ISMRM 14th Scientific Meeting and Exhibition, Seattle, WA. http://afni.nimh.nih.gov/sscc/staff/rwcox/ISMRM_2006/ISMRM%202006%20-%203340/files/02652.pdf)".

Halperin, I., Morelli, M., Korczyn, A.D., Youdim, M.B., Mandel, S.A., 2009. Biomarkers for evaluation of clinical efficacy of multipotential neuroprotective drugs for Alzheimer's and Parkinson's diseases. Neurotherapeutics 6, 128–140.

Hansson, O., Zetterberg, H., Buchhave, P., Londos, E., Blennow, K., Minthon, L., 2006. Association between CSF biomarkers and incipient Alzheimer's disease in patients with mild cognitive impairment: a follow-up study. Lancet Neurol. 5, 228–234.

Henderson, V.W., Buckwalter, J.G., 1994. Cognitive deficits of men and women with Alzheimer's disease. Neurology 44, 90–96.

Herholz, K., Salmon, E., Perani, D., Baron, J.C., Holthoff, V., Frolich, L., Schonknecht, P., Ito, K., Mielke, R., Kalbe, E., Zundorf, G., Delbeuck, X., Pelati, O., Anchisi, D., Fazio, F., Kerrouche, N., Desgranges, B., Eustache, F., Beuthien-Baumann, B., Menzel, C., Schroder, J., Kato, T., Arahata, Y., Henze, M., Heiss, W.D. 2002. Discrimination between Alzheimer dementia and controls by automated analysis of multicenter FDG PET. Neuroimage 17(1), 302–316.

Hill, D., 2010. Neuroimaging to assess safety and efficacy of AD therapies. Expert Opin. Investig. Drugs 19, 23–26.

Ho, A.J., Hua, X., Lee, S., Yanovsky, I., Leow, A.D., Gutman, B., Dinov, I.D., Toga, A.W., Jack, C.R., Jr., Bernstein, M.A., Reiman, E.M., Harvey, D., Kornak, J., Schuff, N., Alexander, G.E., Weiner, M.W., Thompson, P.M. 2009. Comparing 3 T and 1.5 T MRI for tracking Alzheimer's disease progression with tensor-based morphometry. Hum Brain Mapp, 31, 499–514.

Hua, X., Lee, S., Hibar, D.P., Yanovsky, I., Leow, A.D., Toga, A.W., Jack Jr., C.R., Bernstein, M.A., Reiman, E.M., Harvey, D.J., Kornak, J., Schuff, N., Alexander, G.E., Weiner, M.W., Thompson, P.M., Alzheimer's Disease Neuroimaging Initiative, 2010. Mapping Alzheimer's disease progression in 1309 MRI scans: power estimates for different inter-scan intervals. Neuroimage 15, 63–75.

Hua, X., Lee, S., Yanovsky, I., Leow, A.D., Chou, Y.Y., Ho, A.J., Gutman, B., Toga, A.W., Jack, C.R., Jr., Bernstein, M.A., Reiman, E.M., Harvey, D.J., Kornak, J., Schuff, N., Alexander, G.E., Weiner, M.W., Thompson, P.M., Alzheimer's Disease Neuroimaging Initiative, 2009. Optimizing power to track brain degeneration in Alzheimer's disease and mild cognitive impairment with tensor-based morphometry: an ADNI study of 515 subjects. Neuroimage 48, 668–681.

Hua, X., Leow, A.D., Lee, S., Klunder, A.D., Toga, A.W., Lepore, N., Chou, Y.Y., Brun, C., Chiang, M.C., Barysheva, M., Jack, C.R., Jr., Bernstein, M.A., Britson, P.J., Ward, C.P., Whitwell, J.L., Borowski, B., Fleisher, A.S., Fox, N.C., Boyes, R.G., Barnes, J., Harvey, D., Kornak, J., Schuff, N., Boreta, L., Alexander, G.E., Weiner, M.W., Thompson, P.M., Alzheimer's Disease Neuroimaging Initiative, 2008a. 3D characterization of brain atrophy in Alzheimer's disease and mild cognitive impairment using tensor-based morphometry. Neuroimage 41, 19–34.

Hua, X., Leow, A.D., Parikshak, N., Lee, S., Chiang, M.C., Toga, A.W., Jack, C.R., Jr., Weiner, M.W., Thompson, P.M., 2008b. Tensor-based morphometry as a neuroimaging biomarker for Alzheimer's disease: an MRI study of 676 AD, MCI, and normal subjects. Neuroimage 43, 458–469.

Hughes, C.P., Berg, L., Danziger, W.L., Coben, L.A., Martin, R.L., 1982. A new clinical scale for the staging of dementia. Br. J. Psychiatry 140, 566–572.

Ibach, B., Binder, H., Dragon, M., Poljansky, S., Haen, E., Schmitz, E., Koch, H., Putzhammer, A., Kluenemann, H., Wieland, W., Hajak, G., 2006. Cerebrospinal fluid tau and beta-amyloid in Alzheimer patients, disease controls and an age-matched random sample. Neurobiol. Aging 27, 1202–1211.

Jack, C.R., Jr., Petersen, R.C., Xu, Y.C., O'Brien, P.C., Smith, G.E., Ivnik, R.J., Boeve, B.F., Waring, S.C., Tangalos, E.G., Kokmen, E., 1999. Prediction of AD with MRI-based hippocampal volume in mild cognitive impairment. Neurology 52, 1397–1403.

Jack, C.R., Jr., Slomkowski, M., Gracon, S., Hoover, T.M., Felmlee, J.P., Stewart, K., Xu, Y., Shiung, M., O'Brien, P.C., Cha, R., Knopman, D., Petersen, R.C., 2003. MRI as a biomarker of disease progression in a therapeutic trial of milameline for AD. Neurology 60, 253–260.

Jack, C.R., Jr., Shiung, M.M., Gunter, J.L., O'Brien, P.C., Weigand, S.D., Knopman, D.S., Boeve, B.F., Ivnik, R.J., Smith, G.E., Cha, R.H., Tangalos, E.G., Petersen, R.C., 2004. Comparison of different MRI brain atrophy rate measures with clinical disease progression in AD. Neurology 62, 591–600.

Jack, C.R., Jr., Bernstein, M.A., Fox, N.C., Thompson, P., Alexander, G., Harvey, D., Borowski, B., Britson, P.J., J, L.W., Ward, C., Dale, A.M., Felmlee, J.P., Gunter, J.L., Hill, D.L., Killiany, R., Schuff, N., Fox-Bosetti, S., Lin, C., Studholme, C., DeCarli, C.S., Krueger, G., Ward, H.A., Metzger, G.J., Scott, K.T., Mallozzi, R., Blezek, D., Levy, J., Debbins, J.P., Fleisher, A.S., Albert, M., Green, R., Bartzokis, G., Glover, G., Mugler, J., Weiner, M.W., 2008a. The Alzheimer's Disease Neuroimaging Initiative (ADNI): MRI methods. J. Magn. Reson. Imaging 27, 685–691.

Jack, C.R., Jr., Lowe, V.J., Senjem, M.L., Weigand, S.D., Kemp, B.J., Shiung, M.M., Knopman, D.S., Boeve, B.F., Klunk, W.E., Mathis, C.A., Petersen, R.C., 2008b. 11C PiB and structural MRI provide complementary information in imaging of Alzheimer's disease and amnestic mild cognitive impairment. Brain 131, 665–680.

Jack, C.R., Jr., Weigand, S.D., Shiung, M.M., Przybelski, S.A., O'Brien, P.C., Gunter, J.L., Knopman, D.S., Boeve, B.F., Smith, G.E., Petersen, R.C., 2008c. Atrophy rates accelerate in amnestic mild cognitive impairment. Neurology 70, 1740–1752.

Jack, C.R., Jr., Lowe, V.J., Weigand, S.D., Wiste, H.J., Senjem, M.L., Knopman, D.S., Shiung, M.M., Gunter, J.L., Boeve, B.F., Kemp, B.J., Weiner, M., Petersen, R.C., 2009. Serial PIB and MRI in normal, mild cognitive impairment and Alzheimer's disease: implications for sequence of pathological events in Alzheimer's disease. Brain 132, 1355–1365.

Jagust, W.J., Landau, S.M., Shaw, L.M., Trojanowski, J.Q., Koeppe, R.A., Reiman, E.M., Foster, N.L., Petersen, R.C., Weiner, M.W., Price, J.C., Mathis, C.A., 2009. Relationships between biomarkers in aging and dementia. Neurology 73, 1193–1199.

Jovicich, J., Czanner, S., Greve, D., Haley, E., van der Kouwe, A., Gollub, R., Kennedy, D., Schmitt, F., Brown, G., Macfall, J., Fischl, B., Dale, A., 2006. Reliability in multi-site structural MRI studies: effects of gradient non-linearity correction on phantom and human data. Neuroimage 30, 436–443.

Joyner, A.H., J, C.R., Bloss, C.S., Bakken, T.E., Rimol, L.M., Melle, I., Agartz, I., Djurovic, S., Topol, E.J., Schork, N.J., Andreassen, O.A., Dale, A.M., 2009. A common MECP2 haplotype associates with reduced cortical surface area in humans in two independent populations. Proc. Natl. Acad. Sci. U. S. A. 106, 15483–15488.

Karas, G.B., Scheltens, P., Rombouts, S.A., Visser, P.J., van Schijndel, R.A., Fox, N.C., Barkhof, F., 2004. Global and local gray matter loss in mild cognitive impairment and Alzheimer's disease. Neuroimage 23, 708–716.

Leow, A.D., Klunder, A.D., Jack, C.R., Jr., Toga, A.W., Dale, A.M., Bernstein, M.A., Britson, P.J., Gunter, J.L., Ward, C.P., Whitwell, J.L., Borowski, B.J., Fleisher, A.S., Fox, N.C., Harvey, D., Kornak, J., Schuff, N., Studholme, C., Alexander, G.E., Weiner, M.W., Thompson, P.M., 2006. Longitudinal stability of MRI for mapping brain change using tensor-based morphometry. Neuroimage 31, 627–640.

Leow, A.D., Yanovsky, I., Parikshak, N., Hua, X., Lee, S., Toga, A.W., Jack, C.R., Jr., Bernstein, M.A., Britson, P.J., Gunter, J.L., Ward, C.P., Borowski, B., Shaw, L.M., Trojanowski, J.Q., Fleisher, A.S., Harvey, D., Kornak, J., Schuff, N., Alexander, G.E., Weiner, M.W., Thompson, P.M., 2009. Alzheimer's disease neuroimaging initiative: a one-year follow up study using tensor-based morphometry correlating degenerative rates, biomarkers and cognition. Neuroimage 45, 645–655.

Macintyre, S., Hunt, K., Sweeting, H., 1996. Gender differences in health: are things really as simple as they seem? Soc. Sci. Med. 42, 617–624.

Mazziotta, J., Toga, A., Evans, A., Fox, P., Lancaster, J., Zilles, K., Woods, R., Paus, T., Simpson, G., Pike, B., Holmes, C., Collins, L., Thompson, P., MacDonald, D., Iacoboni, M., Schormann, T., Amunts, K., Palomero-Gallagher, N., Geyer, S., Parsons, L., Narr, K., Kabani, N., Le Goualher, G., Boomsma, D., Cannon, T., Kawashima, R., Mazoyer, B., 2001. A probabilistic atlas and reference system for the human brain: International Consortium for Brain Mapping (ICBM). Philos. Trans. R. Soc. Lond. B Biol. Sci. 356, 1293–1322.

McKhann, G., Drachman, D., Folstein, M., Katzman, R., Price, D., Stadlan, E.M., 1984. Clinical diagnosis of Alzheimer's disease: report of the NINCDS-ADRDA Work Group under the auspices of Department of Health and Human Services Task Force on Alzheimer's Disease. Neurology 34, 939–944.

Misra, C., Fan, Y., Davatzikos, C., 2009. Baseline and longitudinal patterns of brain atrophy in MCI patients, and their use in prediction of short-term conversion to AD: results from ADNI. Neuroimage 44, 1415–1422.

Mohs, R.C., 1994. Administration and Scoring Manual for the Alzheimer's Disease Assessment Scale, 1994 Revised Edition. The Mount Sinai School of Medicine, New York.

Moreno-Martinez, F.J., Laws, K.R., Schulz, J., 2008. The impact of dementia, age and sex on category fluency: greater deficits in women with Alzheimer's disease. Cortex 44, 1256–1264.

Morra, J.H., Tu, Z., Apostolova, L.G., Green, A.E., Avedissian, C., Madsen, S.K., Parikshak, N., Hua, X., Toga, A.W., Jack, C.R., Jr., Schuff, N., Weiner, M.W., Thompson, P.M., 2009a. Automated 3D mapping of hippocampal atrophy and its clinical correlates in 400 subjects with Alzheimer's disease, mild cognitive impairment, and elderly controls. Hum. Brain Mapp. 30, 2766–2788.

Morra, J.H., Tu, Z., Apostolova, L.G., Green, A.E., Avedissian, C., Madsen, S.K., Parikshak, N., Toga, A.W., Jack, C.R., Jr., Schuff, N., Weiner, M.W., Thompson, P.M., 2009b. Automated mapping of hippocampal atrophy in 1-year repeat MRI data from 490 subjects with Alzheimer's disease, mild cognitive impairment, and elderly controls. Neuroimage 45, S3–S15.

Morris, J.C., 1993. The Clinical Dementia Rating (CDR): current version and scoring rules. Neurology 43, 2412–2414.

Mortimer, J.A., Borenstein, A.R., Gosche, K.M., Snowdon, D.A., 2005. Very early detection of Alzheimer neuropathology and the role of brain reserve in modifying its clinical expression. J. Geriatr. Psychiatry Neurol. 18, 218–223.

Mueller, S.G., Schuff, N., Weiner, M.W., 2006. Evaluation of treatment effects in Alzheimer's and other neurodegenerative diseases by MRI and MRS. NMR Biomed. 19, 655–668.

Mueller, S.G., Weiner, M.W., Thal, L.J., Petersen, R.C., Jack, C., Jagust, W., Trojanowski, J.Q., Toga, A.W., Beckett, L., 2005a. The Alzheimer's Disease Neuroimaging Initiative. Neuroimaging Clin. N. Am. 15, 869–877, xi–xii.

Mueller, S.G., Weiner, M.W., Thal, L.J., Petersen, R.C., Jack, C.R., Jagust, W., Trojanowski, J.Q., Toga, A.W., Beckett, L., 2005b. Ways toward an early diagnosis in Alzheimer's disease: The Alzheimer's Disease Neuroimaging Initiative (ADNI). Alzheimers Dement. 1, 55–66.

Nestor, S.M., Rupsingh, R., Borrie, M., Smith, M., Accomazzi, V., Wells, J.L., Fogarty, J., Bartha, R., 2008. Ventricular enlargement as a possible measure of Alzheimer's disease progression validated using the Alzheimer's disease neuroimaging initiative database. Brain 131, 2443–2454.

Ngandu, T., von Strauss, E., Helkala, E.L., Winblad, B., Nissinen, A., Tuomilehto, J., Soininen, H., Kivipelto, M., 2007. Education and dementia: what lies behind the association? Neurology 69, 1442–1450.

Paling, S.M., Williams, E.D., Barber, R., Burton, E.J., Crum, W.R., Fox, N.C., O'Brien, J.T., 2004. The application of serial MRI analysis techniques to the study of cerebral atrophy in late-onset dementia. Med. Image Anal. 8, 69–79.

Petersen, R.C., 2003. Mild Cognitive Impairment: Aging to Alzheimer's Disease. Oxford University Press, New York.

Petersen, R.C., Doody, R., Kurz, A., Mohs, R.C., Morris, J.C., Rabins, P.V., Ritchie, K., Rossor, M., Thal, L., Winblad, B., 2001. Current concepts in mild cognitive impairment. Arch. Neurol. 58, 1985–1992.

Pfeffer, R.I., Kurosaki, T.T., Harrah, C.H., Jr., Chance, J.M., Filos, S., 1982. Measurement of functional activities in older adults in the community. J. Gerontol. 37, 323–329.

Pievani, M., Rasser, P.E., Galluzzi, S., Benussi, L., Ghidoni, R., Sabattoli, F., Bonetti, M., Binetti, G., Thompson, P.M., Frisoni, G.B., 2009. Mapping the effect of APOE epsilon4 on gray matter loss in Alzheimer's disease in vivo. Neuroimage 45, 1090–1098.

Potkin, S.G., Guffanti, G., Lakatos, A., Turner, J.A., Kruggel, F., Fallon, J.H., Saykin, A.J., Orro, A., Lupoli, S., Salvi, E., Weiner, M., Macciardi, F., 2009. Hippocampal atrophy as a quantitative trait in a genome-wide association study identifying novel susceptibility genes for Alzheimer's disease. PLoS One 4, e6501.

Purcell, S., Neale, B., Todd-Brown, K., Thomas, L., Ferreira, M.A., Bender, D., Maller, J., Sklar, P., de Bakker, P.I., Daly, M.J., Sham, P.C., 2007. PLINK: a tool set for whole-genome association and population-based linkage analyses. Am. J. Hum. Genet. 81, 559–575.

Raji, C.A., Ho, A.J., Parikshak, N.N., Becker, J.T., Lopez, O.L., Kuller, L.H., Hua, X., Leow, A.D., Toga, A.W., Thompson, P.M., 2010. Brain structure and obesity. Hum. Brain. Mapp. 31, 353–364.

Rey, A., 1964. L'examen clinique en psychologie. Presses Universitaires de France, Paris.

Riddle, W.R., Li, R., Fitzpatrick, J.M., DonLevy, S.C., Dawant, B.M., Price, R.R., 2004. Characterizing changes in MR images with color-coded Jacobians. Magn. Reson. Imaging 22, 769–777.

Ridha, B.H., Barnes, J., Bartlett, J.W., Godbolt, A., Pepple, T., Rossor, M.N., Fox, N.C., 2006. Tracking atrophy progression in familial Alzheimer's disease: a serial MRI study. Lancet Neurol. 5, 828–834.

Risacher, S.L., Saykin, A.J., West, J.D., Shen, L., Firpi, H.A., McDonald, B.C., 2009. Baseline MRI predictors of conversion from MCI to probable AD in the ADNI cohort. Curr. Alzheimer Res. 6, 347–361.

Rosen, W.G., Mohs, R.C., Davis, K.L., 1984. A new rating scale for Alzheimer's disease. Am. J. Psychiatry 141, 1356–1364.

Roses, A.D., 1996. Apolipoprotein E alleles as risk factors in Alzheimer's disease. Annu. Rev. Med. 47, 387–400.

Roses, A.D., Saunders, A.M., 1994. APOE is a major susceptibility gene for Alzheimer's disease. Curr. Opin. Biotechnol. 5, 663–667.

Roses, A.D., Saunders, A.M., Alberts, M.A., Strittmatter, W.J., Schmechel, D., Gorder, E., Pericak-Vance, M.A., 1995. Apolipoprotein E E4 allele and risk of dementia. JAMA 273, 374–375.

Rosner, B., 1990. Fundamentals of Biostatistics. PWS-Kent Publishing Company, Boston.

Saunders, A.M., Strittmatter, W.J., Schmechel, D., George-Hyslop, P.H., Pericak-Vance, M.A., Joo, S.H., Rosi, B.L., Gusella, J.F., Crapper-MacLachlan, D.R., Alberts, M.J., et al., 1993. Association of apolipoprotein E allele epsilon 4 with late-onset familial and sporadic Alzheimer's disease. Neurology 43, 1467–1472.

Scahill, R.I., Schott, J.M., Stevens, J.M., Rossor, M.N., Fox, N.C., 2002. Mapping the evolution of regional atrophy in Alzheimer's disease: unbiased analysis of fluid-registered serial MRI. Proc. Natl. Acad. Sci. U. S. A. 99, 4703–4707.

Scahill, R.I., Frost, C., Jenkins, R., Whitwell, J.L., Rossor, M.N., Fox, N.C., 2003. A longitudinal study of brain volume changes in normal aging using serial registered magnetic resonance imaging. Arch. Neurol. 60, 989–994.

Scarmeas, N., Albert, S.M., Manly, J.J., Stern, Y., 2006. Education and rates of cognitive decline in incident Alzheimer's disease. J. Neurol. Neurosurg. Psychiatry 77, 308–316.

Schuff, N., Woerner, N., Boreta, L., Kornfield, T., Shaw, L.M., Trojanowski, J.Q., Thompson, P.M., Jack, C.R., Jr., Weiner, M.W., 2009. MRI of hippocampal volume loss in early Alzheimer's disease in relation to ApoE genotype and biomarkers. Brain 132, 1067–1077.

Selkoe, D.J., 2004. Cell biology of protein misfolding: the examples of Alzheimer's and Parkinson's diseases. Nat. Cell Biol. 6, 1054–1061.

Shaw, L.M., Korecka, M., Clark, C.M., Lee, V.M., Trojanowski, J.Q., 2007. Biomarkers of neurodegeneration for diagnosis and monitoring therapeutics. Nat. Rev. 6, 295–303.

Skovronsky, D.M., Lee, V.M., Trojanowski, J.Q., 2006. Neurodegenerative diseases: new concepts of pathogenesis and their therapeutic implications. Annu. Rev. Pathol. 1, 151–70.

Sled, J.G., Zijdenbos, A.P., Evans, A.C., 1998. A nonparametric method for automatic correction of intensity nonuniformity in MRI data. IEEE Trans. Med. Imaging 17, 87–97.

Sluimer, J.D., van der Flier, W.M., Karas, G.B., Fox, N.C., Scheltens, P., Barkhof, F., Vrenken, H., 2008. Whole-brain atrophy rate and cognitive decline: longitudinal MR study of memory clinic patients. Radiology 248, 590–598.

Sluimer, J.D., van der Flier, W.M., Karas, G.B., van Schijndel, R., Barnes, J., Boyes, R.G., Cover, K.S., Olabarriaga, S.D., Fox, N.C., Scheltens, P., Vrenken, H., Barkhof, F., 2009. Accelerating regional atrophy rates in the progression from normal aging to Alzheimer's disease. Eur. Radiol. 19, 2826–2833.

Smith, A.D., Jobst, K.A., 1996. Use of structural imaging to study the progression of Alzheimer's disease. Br. Med. Bull. 52, 575–586.

Smith, A.D., 2002. Imaging the progression of Alzheimer pathology through the brain. 99, 4135–4137.Proc. Natl. Acad. Sci. U. S. A.

Smith, S.M., Jenkinson, M., Woolrich, M.W., Beckmann, C.F., Behrens, T.E., Johansen-Berg, H., Bannister, P.R., De Luca, M., Drobnjak, I., Flitney, D.E., Niazy, R.K., Saunders, J., Vickers, J., Zhang, Y., De Stefano, N., Brady, J.M., Matthews, P.M., 2004. Advances in functional and structural MR image analysis and implementation as FSL. Neuroimage 23, S208–S219.

Smith, S.M., Zhang, Y., Jenkinson, M., Chen, J., Matthews, P.M., Federico, A., De Stefano, N., 2002. Accurate, robust, and automated longitudinal and cross-sectional brain change analysis. Neuroimage 17, 479–489.

Stein, J.L., Hua, X., Morra, J.H., Lee, S., Hibar, D.P., Ho, A.J., Leow, A.D., Toga, A.W., Sul, J.H., Kang, H., Eskin, E., Saykin, A.J., Shen, L., Foroud, T., Pankratz, N., Huentelman, M.J., Craig, D.W., Gerber, J.D., Allen, A.N., Corneveaux, J.J., Stephan, D.A., Webster, J., DeChairo, B.M., Potkin, S.G., Jack, C.R., Weiner, M.W., Thompson, P.M., 2010. Genome-wide analysis reveals novel genes influencing temporal lobe structure with relevance to neurodegeneration in Alzheimer's disease. submitted.

Storey, J.D., 2002. A direct approach to false discovery rates. J. R. Stat. Soc. B 64, 479–498.

Thal, L.J., Kantarci, K., Reiman, E.M., Klunk, W.E., Weiner, M.W., Zetterberg, H., Galasko, D., Pratico, D., Griffin, S., Schenk, D., Siemers, E., 2006. The role of biomarkers in clinical trials for Alzheimer disease. Alzheimer Dis. Assoc. Disord. 20, 6–15.

Thompson, P.M., Giedd, J.N., Woods, R.P., MacDonald, D., Evans, A.C., Toga, A.W., 2000. Growth patterns in the developing brain detected by using continuum mechanical tensor maps. Nature 404, 190–193.

Thompson, P.M., Hayashi, K.M., de Zubicaray, G., Janke, A.L., Rose, S.E., Semple, J., Herman, D., Hong, M.S., Dittmer, S.S., Doddrell, D.M., Toga, A.W., 2003. Dynamics of gray matter loss in Alzheimer's disease. J. Neurosci. 23, 994–1005.

Thompson, P.M., Hayashi, K.M., De Zubicaray, G.I., Janke, A.L., Rose, S.E., Semple, J., Hong, M.S., Herman, D.H., Gravano, D., Doddrell, D.M., Toga, A.W., 2004. Mapping hippocampal and ventricular change in Alzheimer disease. Neuroimage 22, 1754–1766.

Toga, A.W., 1999. Brain Warping. Academic Press, San Diego.

Tower, J., 2006. Sex-specific regulation of aging and apoptosis. Mech. Ageing Dev. 127, 705–718.

Tower, J., Arbeitman, M., 2009. The genetics of gender and life span. J. Biol. 8, 38.

Vemuri, P., Whitwell, J.L., Kantarci, K., Josephs, K.A., Parisi, J.E., Shiung, M.S., Knopman, D.S., Boeve, B.F., Petersen, R.C., Dickson, D.W., Jack, C.R., Jr., 2008. Antemortem MRI based STructural Abnormality iNDex (STAND)-scores correlate with postmortem Braak neurofibrillary tangle stage. Neuroimage 42, 559–567.

Vemuri, P., Wiste, H.J., Weigand, S.D., Shaw, L.M., Trojanowski, J.Q., Weiner, M.W., Knopman, D.S., Petersen, R.C., Jack, C.R., Jr., 2009. MRI and CSF biomarkers in normal, MCI, and AD subjects: predicting future clinical change. Neurology 73, 294–301.

Wechsler, D., 1987. WMS-R Wechsler Memory Scale - Revised Manual. The Psychological Corporation, Harcourt Brace Jovanovich, Inc., New York.

Whitwell, J.L., Przybelski, S.A., Weigand, S.D., Knopman, D.S., Boeve, B.F., Petersen, R.C., Jack, C.R., Jr., 2007. 3D maps from multiple MRI illustrate changing atrophy patterns as subjects progress from mild cognitive impairment to Alzheimer's disease. Brain 130, 1777–1786.

Whitwell, J.L., Josephs, K.A., Murray, M.E., Kantarci, K., Przybelski, S.A., Weigand, S.D., Vemuri, P., Senjem, M.L., Parisi, J.E., Knopman, D.S., Boeve, B.F., Petersen, R.C., Dickson, D.W., Jack, C.R., Jr., 2008. MRI correlates of neurofibrillary tangle pathology at autopsy: a voxel-based morphometry study. Neurology 71, 743–749.

Yanovsky, I., Leow, A.D., Lee, S., Osher, S.J., Thompson, P.M., 2009. Comparing registration methods for mapping brain change using tensor-based morphometry. Med. Image Anal. 13, 679–700.